Title

The kinetics of solid-state isotope-exchange reactions for clumped isotopes: A study of inorganic calcites and apatites from natural and experimental samples

Journal

American Journal of Science, 315(5)

ISSN

0002-9599

Authors

Stolper, DA
Eiler, JM

Publication Date

2015-05-01

DOI

10.2475/05.2015.01

Peer reviewed

The kinetics of solid-state isotope-exchange reactions for clumped isotopes: A study of inorganic calcites and apatites from natural and experimental samples

Daniel A. Stolper[*,†] **and John M. Eiler**[*]

[*] Division of Geological and Planetary Sciences, California Institute of Technology, Pasadena, California 91125, USA

[*] Division of Geological and Planetary Sciences, California Institute of Technology, Pasadena, California 91125, USA

[†] Corresponding author's present address: Department of Geosciences, Princeton University, Princeton, New Jersey 08544; dstolper@princeton.edu

Abstract

Carbonate clumped-isotope geothermometry is a tool used to reconstruct formation or (re)equilibration temperatures of carbonate bearing minerals, including carbonate groups substituted into apatite. It is based on the preference for isotopologues with multiple heavy isotopes (for example, $^{13}C^{16}O_2{}^{18}O^{2-}$groups) to be more abundant at equilibrium than would be expected if all isotopes were randomly distributed amongst all carbonate groups. Because this preference is only a function of temperature, excesses of multiply substituted species can be used to calculate formation temperatures without knowledge of the isotopic composition of water from which the mineral precipitated or other phases with which it may have equilibrated. However, the measured temperature could be modified after mineral growth if exchange of isotopes amongst carbonate groups within the mineral has occurred through internal isotope-exchange reactions. Because these exchange reactions occur through thermally activated processes, their rates depend on temperature and increase at higher temperatures. Thus internal isotope-exchange reactions could lead to effective re-equilibration at high temperatures, overprinting the original temperatures recorded during mineral growth. We measured clumped-isotope temperatures in carbonate bearing minerals (including apatites) from several carbonatites to constrain the kinetics of these internal isotope-exchange reactions. We observe two key trends for clumped-isotope temperatures in carbonatites: (*i*) clumped-isotope temperatures of apatites and carbonate-bearing minerals decrease with increasing intrusion depth and (*ii*) apatites record lower clumped-isotope temperatures than carbonate minerals from the same intrusion. We additionally conducted heating experiments at different temperatures to derive the temperature dependence for the rate constants that describe the alteration of clumped-isotope temperatures with time in calcites and apatites. We find that calcites exhibit complex kinetics as has been seen in previous studies. To quantify these results, we constructed a model that incorporates both diffusion of isotopes through the crystal lattice and isotope-exchange reactions between adjacent carbonate groups. We tested this model through comparison to previous measurements of optical calcites and brachiopods and to samples with known cooling histories and find that the model is able to reasonably capture kinetic data from previous experiments and the observed clumped-isotope temperatures of calcites assuming geologically reasonable cooling rates. A similar model for apatite over-predicts the observed clumped-isotope temperatures found in natural samples; we hypothesize this discrepancy is the result of annealing of radiation damage in our experiments, which lowers the diffusivity and rate of isotope exchange of carbonate groups compared to damaged natural samples. Finally, we constructed models to explore how heating can alter recorded clumped-isotope temperatures. Our model predicts that samples change in clumped-isotope temperatures in two stages. The first stage changes the recorded clumped isotope temperatures by <1 °C if held at 75 °C for 100 million years and by up to ~40 °C if held at 120 °C, but the clumped-isotope temperatures does not reach ambient values through this low-temperature mechanism. A second, slower change becomes effective at temperatures above 150 °C and can take the measured clumped-isotope temperature up to the true ambient temperature. This result implies that old (hundreds of million years) samples that have only experienced mild (<100-125 °C) thermal histories could exhibit small but measurable (order 10 °C) changes in their clumped-isotope temperatures. We compared this heating model to clumped-isotope measurements from paleosol samples from the Siwalik Basin in Nepal, which were buried up to 5 km and then rapidly exhumed to the surface; these samples often do not give reasonable surface temperatures. The modeled temperatures agree with measured temperatures of these samples, suggesting that partial re-equilibration during shallow crustal burial is responsible for their elevated clumped-isotope temperatures.

INTRODUCTION

The carbonate 'clumped-isotope' geothermometer (Ghosh and others, 2006) provides a method for measuring formation temperatures of carbonate-bearing minerals formed at isotopic equilibrium. It is based on the thermodynamic preference for carbonate groups with two or more heavy isotopes (for example, $^{13}C^{16}O_2{}^{18}O^{2-}$), which we term 'clumped' isotopologues, to be enriched compared to a random ordering of isotopes amongst all carbonate isotopologues (Schauble and others, 2006). This enrichment is a measureable function of temperature (Ghosh and others, 2006; Dennis and Schrag, 2010; Zaarur and others, 2013) and thus can serve as a geothermometer for carbonate formation in minerals such as calcite, aragonite, and dolomite, as well as carbonate groups in apatite (Ghosh and others, 2006; Eagle and others, 2010; Ferry and others, 2011; Lloyd and Eiler, 2014).

The carbonate clumped-isotope geothermometer is distinct from many other low-temperature (<~300 °C) isotopic geothermometers because the measured formation temperature is independent of the isotopic composition of the water from which the carbonate-bearing mineral crystallized. That is, most isotopic geothermometers are based on heterogeneous phase equilibrium isotope-exchange reactions that require the isotopic composition of at least two phases to be known. The classic example of such is the ^{18}O carbonate-water geothermometer, which is based on differences in $^{18}O/^{16}O$ ratios of carbonate minerals and water (Urey, 1947; McCrea, 1950; Epstein and others, 1953). In contrast, clumped-isotope-based geothermometers, of which the carbonate clumped-isotope geothermometer is just a single example (for example, Wang and others, 2004; Yeung and others, 2012; Stolper and others, 2014), are based on homogeneous phase isotope-exchange reactions — in other words the isotopic composition of only a single phase is required to reconstruct paleotemperatures. An example of such an isotope-exchange reaction in carbonates is:

$$Ca^{12}C^{16}O_3 + Ca^{13}C^{16}O_2{}^{18}O \leftrightarrow Ca^{12}C^{16}O_2{}^{18}O + Ca^{13}C^{16}O_3. \quad (1)$$

The equilibrium constant for the reaction in equation (1) is a function of temperature and favors the left side of the equation at all finite temperatures (Schauble and others, 2006). Critically, for this reaction, only the isotopic composition of a carbonate mineral is needed for paleotemperature reconstructions. This is significant because, although carbonate-bearing marine rocks exist for most of the rock record (~billions of years; for example, Jaffrés and others, 2007), there are few instances in which carbonates from the geological record can be directly compared to the waters from which they precipitated. Although many estimates and models of the isotopic composition of ancient waters exist, this subject remains controversial (for example, Muehlenbachs, 1986; Lécuyer and Allemand, 1999; Veizer and others, 1999; Kasting and others, 2006; Jaffrés and others, 2007). Consequently, carbonate clumped-isotope geothermometry creates the opportunity to reconstruct past surface temperatures using the large number of ancient rocks that contain carbonate-bearing minerals (for example, Came and others, 2007; Finnegan and others, 2011; Keating-Bitonti and others, 2011; Dennis and others, 2013; Price and Passey, 2013; Snell and others, 2013; Cummins and others, 2014; Douglas and others, 2014).

Although the study of clumped isotopes in carbonates offers great promise to many geological problems, a critical issue is understanding how well minerals retain their original clumped-isotope signature after formation. Isotopic clumping in carbonates is susceptible to resetting from recrystallization, open-system isotope-exchange reactions (that is, where the crystal lattice undergoes mass transfer reactions with the outside environment), and reordering through closed-system isotope-exchange reactions in which C--O bonds within a mineral are broken and re-formed (fig. 1; Ghosh and others, 2006; Dennis and Schrag, 2010; Eiler, 2011; Passey and Henkes, 2012; Henkes and others, 2014). In this respect, the carbonate clumped-isotope geothermometer most resembles petrologic geothermometers based on homogenous phase order-disorder reactions, such as the ordering of iron and magnesium on the M1 and M2 sites in orthopyroxenes (Zhang, 2008). If any of these processes has occurred in a sample, the temperature measured through the clumped-isotope thermometer will not reflect the original formation temperature of the mineral. On the other hand, if these processes and their effects on the isotopic

ordering of carbonates are well understood, clumped-isotope temperatures could provide a new tool for studying the thermal and diagenetic histories of shallow crustal rocks (for example, Eiler, 2011; Passey and Henkes, 2012; Henkes and others, 2014). Interpretations of measured temperatures require a quantitative knowledge of the kinetics of recrystallization and both open- and closed-system isotope-exchange reactions. We focus here on understanding the kinetics of closed-system isotope-exchange reactions, expanding on studies of Ghosh and others (2006), Dennis and Schrag (2010), Passey and Henkes (2012), and Henkes and others (2014).

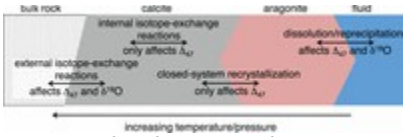

View larger version:

- In this page
- In a new window

Fig. 1.
Cartoon representation of various processes that can cause $\delta^{18}O$ and/or Δ_{47}values of a mineral to change.

Background on Previous Investigations of the Kinetics of Closed-System Isotope-Exchange Reactions in Calcite

The kinetics of closed-system solid-state isotope-exchange reactions for clumped isotopes in carbonates were first addressed by Ghosh and others (2006)who measured clumped-isotope temperatures of calcite from two Italian marbles. These marbles returned temperatures of ~200 °C. This temperature is below the maximum metamorphic temperatures reached by these rocks (upper greenschist facies; Ghosh and others, 2006). As concluded by Ghosh and others (2006), these results indicate that the clumped-isotope temperatures of 'high-temperature' rocks such as marbles record 'apparent or fictive temperatures' (for example, Zhang, 2008) that are neither related to the formation temperature of the original minerals nor the recrystallization or maximum burial temperature of the marble. Instead these temperatures are more similar to 'closure' temperatures (Dodson, 1973) commonly observed in radiogenic isotope systems and reflect the thermal history of the rock (fig. 2). 'Closure temperature' is arguably not a suitable term for clumped-isotope temperature studies as it implies the retention of some component that could potentially escape when a mineral is 'open' to diffusion. Consequently, we instead define an "apparent equilibrium blocking temperature" as the measured clumped-isotope temperature for a system cooling from high temperatures below which internal reordering by closed-system isotope-exchange reactions becomes so slow that equation (1) ceases to proceed in either the forward or backward direction in any measureable way (fig. 2). Following Zhang (1994), when measured temperatures do not refer to a specific process (for example, formation or blocking), they are generically referred to as "apparent equilibrium temperatures."

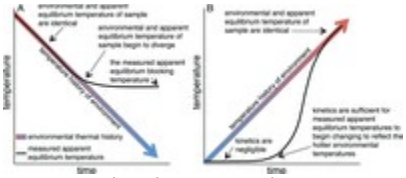

View larger version:

- In this page
- In a new window

Fig. 2.
Cartoon representation of the effects of heating and cooling on measured apparent equilibrium temperatures based on the measured Δ_{47} values. We note that these cartoons are approximations of the real behavior of the system and the curves can have differing shapes depending on the prior thermal history of the samples as well as the heating/cooling rate of the system. (A) A schematic representation of the temperature recorded by the clumped-isotope thermometer (apparent equilibrium temperature) vs. the actual environmental temperature for a system

originally starting at high temperature and cooling. At the start of the history both the environmental and recorded apparent equilibrium temperature are identical. At a lower temperature the kinetics of exchange and diffusion slow sufficiently causing the recorded apparent equilibrium temperature to lock in, which is termed the "apparent equilibrium blocking temperature." (B) A schematic representation of the temperature recorded by the apparent equilibrium temperature vs. the actual environmental temperature for a system originally starting at low temperature and heated to higher temperatures. As the environmental temperature initially rises, the recorded apparent equilibrium temperature does not change. Only until the environment reaches a threshold temperature does the apparent equilibrium temperature being to change in a measurable way. At first the kinetics are not sufficient for the apparent equilibrium temperatures to catch up to the environmental temperature, which occurs at a higher temperature (or after a sufficient amount of time).

Dennis and Schrag (2010) expanded on the work of Ghosh and others (2006)through the measurement of apparent equilibrium blocking temperatures recorded by carbonate minerals in carbonatites. Carbonatites are igneous rocks containing greater than 50 modal percent carbonate minerals (Mitchell, 2005). These rocks crystallize from melts at high (~650 °C) temperatures (Wyllie and Tuttle, 1960). Generally, carbonatites preserved in the geological record are intrusive and, consequently, cooled over geologically relevant time scales (for example, millions of years). They found that carbonate minerals from carbonatites generally record apparent equilibrium blocking temperatures between ~100 °C to 300 °C — lower than the crystallization temperatures of carbonatites and thus in at least loose agreement with the results of Ghosh and others (2006) for marbles. These results give a general guide to the apparent equilibrium blocking temperatures of calcite with respect to equation (1). However, it is not obvious whether these temperatures reflect the kinetics of internal isotope-exchange reactions alone or might also be influenced by recrystallization or open-system isotope-exchange reactions. More generally, without quantitative knowledge of the actual reaction kinetics as a function of temperature, it is difficult to predict the temperatures and, equally importantly, the time at those temperatures needed to measurably modify recorded apparent equilibrium temperatures.

A quantitative framework to describe the kinetics of isotope exchange within calcite was determined experimentally for optical calcite and spar calcite by Passey and Henkes (2012) and brachiopods by Henkes and others (2014). These experiments yield complex, but consistent systematics in which experimental heating leads to a two-phased change in the measured apparent equilibrium temperature of the sample. Specifically, there are relatively rapid (minutes to hours) changes in the measured apparent equilibrium temperature at the start of the experiment and slower (hours to days) changes towards the end that, together, cannot be described by simple pseudo-first-order kinetics of a single chemical reaction. Passey and Henkes (2012) and Henkes and others (2014)created a model to describe these non-pseudo-first-order behaviors as the result of the presence of defects in the crystals that allow for 'fast' exchange paths, but anneal away during the course of the experiments until slower exchange processes become rate-limiting.

The model of Henkes and others (2014) allows for the extraction of kinetic parameters using all data in the experiments and, assuming the kinetic parameters are Arrhenian, extrapolation of the kinetics of isotope-exchange reactions measured at elevated laboratory temperatures to those at lower temperatures relevant for geological thermal histories. This model predicts that for geologically relevant thermal histories that remain below ~150 °C there is no important difference between models that incorporate these defects and those that only incorporate kinetics derived from the second, kinetically 'slower' portion of the experiments. As a result, Henkes and others (2014) did not incorporate the initial, faster kinetics into their models used to understand the thermal histories of natural samples with burial temperatures below ~150 °C. Intriguingly, the optical calcite and brachiopods yield similar (if not indistinguishable) kinetic parameters in the defect-annealing model for both the faster and slower stages of the changes in clumped-isotope values (Henkes and others, 2014).

Clumped Isotopes and Apatites

Most studies of the carbonate clumped-isotope geothermometer thus far have focused on calcite, aragonite, and dolomite. However, an additional mineral of interest to paleoclimate, paleobiology, and petrology that is amenable to clumped-isotope analyses is apatite (Eagle and others, 2010; Eagle and others, 2011). Apatites can be used for clumped-isotope measurements because they can contain carbonate groups dissolved in their mineral structure. These carbonate groups can be analyzed for both bulk- and clumped-isotope compositions via acid-digestion release of CO_2 (Kolodny and Kaplan, 1970; Eagle and others, 2010).

Carbonate groups in apatite substitutes for either phosphate groups or F, Cl and OH groups (Silverman and others, 1952; McClellan, 1980). Apatites are useful for temperature reconstructions for both paleoclimate and paleobiology because many organisms make their skeletons or teeth out of apatite. Additionally, apatite is a common constituent in igneous, metamorphic and sedimentary rocks. Finally, apatites may undergo diagenesis differently from carbonate minerals, and therefore could provide a useful point of comparison to deconvolve post-depositional changes to clumped-isotope signatures (Shemesh and others, 1983; Shemesh and others, 1988; Longinelli and others, 2003). For example, a potentially useful check on paleotemperature reconstructions is the comparison of temperatures derived via clumped-isotope analyses from carbonate groups in both apatites and carbonate minerals from the same lithological unit.

There currently exists no estimate for the apparent equilibrium blocking temperature of carbonate groups in apatites for clumped-isotope measurements — this information is needed to put such a comparison into context. Fossil dinosaur teeth yield maximum apparent equilibrium temperatures of ~80 to 100 °C, which must be the result of some modification after original mineral growth because these temperatures are too hot for animal survival (Eagle and others, 2011). Although it is not known whether recrystallization associated with diagenesis or closed-system isotope-exchange reactions caused these high temperatures, they imply that the apparent equilibrium blocking temperature for apatite during geologically slow cooling or heating is at least ~80 to 100 °C.

This Study

In order to add further constraints to the kinetics of formation and destruction of multiply substituted carbonate groups in both calcite and apatite, we measured apparent equilibrium temperatures of igneous calcite and apatite samples from the same intrusion from three carbonatite bodies. Additionally, we performed heating experiments on natural optical calcite from Mexico and carbonate-bearing apatite from the Siilinjarvi carbonatite (Finland). To fit the experimental results, we develop a model different from the defect-annealing model proposed by Passey and Henkes (2012) and Henkes and others (2014). This model explains the two-phased nature of the experiments as a consequence of the probability of finding carbonate isotopologues in the correct configuration in the mineral lattice to generate or destroy clumped isotopologues. We demonstrate that our experimental results as well as the results from the optical calcites from Passey and Henkes (2012) and brachiopods from Henkes and others (2014) yield indistinguishable kinetic relationships when fit to this model. We use this model to extrapolate the experimental measurements to lower temperature in order to explore how our model predicts the apparent equilibrium blocking temperature of carbonate-bearing minerals with independently known cooling histories from high-temperature igneous and metamorphic systems. Finally, we model hypothetical time-temperature heating paths to better understand the responses of apparent equilibrium temperatures to thermal perturbations, and compare our model to measured paleosol samples from the Siwalik basin that experienced a relatively simple, well-constrained thermal history.

THEORY AND NOMENCLATURE

Here we briefly review the theory and nomenclature of carbonate clumped-isotope thermometry used in this paper. This material is presented in greater detail in Eiler (2007) and Eiler (2011) and references therein. The critical feature of clumped-isotope geothermometry is that the left side of equation (1) (which has $^{13}C^{16}O_2{}^{18}O^{2-}$) is thermodynamically favored over the right side at all finite temperatures. This results in an excess of multiply substituted isotopologues compared to a random (stochastic) distribution at any finite temperature for an isotopically equilibrated system.

We do not probe equation (1) directly in current clumped-isotope measurements. Instead, we measure the distribution of isotopes amongst isotopologues of CO_2released from carbonate minerals via a phosphoric acid digestion (Ghosh and others, 2006; Guo and others, 2009). The concentration of multiply substituted CO_2 isotopologues at mass 47 (a combination of $^{13}C^{16}O^{18}O$, $^{12}C^{17}O^{18}O$, and $^{13}C^{17}O_2$) released from carbonates relative to the expected random distribution of atoms is largely controlled (~97%) by the equilibrium constant for equation (1). Thus, the amount of mass 47 CO_2 isotopologues relative to a random distribution of isotopes is proportional to temperature in carbonates that form in equilibrium (Ghosh and others, 2006). The details of how CO_3^{2-} groups are converted to CO_2 and considerations regarding this conversion for clumped-isotope measurements is given in Ghosh and others (2006) and Guo and others (2009).

We represent the degree of isotopic ordering (that is, the relative enrichment in clumped isotopologues) in CO_2 extracted from carbonate ions via the Δ_{47}notation where

$$\Delta_{47} = \left(\frac{^{47}R}{^{47}R^*} - 1\right)*1000 - \left(\frac{^{46}R}{^{46}R^*} - 1\right)*1000 - \left(\frac{^{45}R}{^{45}R^*} - 1\right)*1000$$

(Ghosh and others, 2006, Wang and others, 2004). (2)

Here, $^{i}R=[^{i}CO_2]/[^{44}CO_2]$, where the 'i' refers to the cardinal mass of the isotopologue (or isotopologues) of interest. For example $^{44}CO_2$ is equivalent to $^{12}C^{16}O_2$ while $^{45}CO_2$ includes both $^{13}C^{16}O_2$ and $^{12}C^{16}O^{17}O$. The superscript * refers to a system that has the same bulk isotopic content as the sample but a random distribution of isotopes amongst all isotopologues.

METHODS

Isotopic Measurements

~8 mg (±2) of calcite and 100 to 500 mg of apatite were used for each sample analysis. Samples, if not already powdered (as in the case of standards used), were hand crushed (dry) with an agate mortar and pestle. CO_2 was extracted on one of two custom made (and nearly identical) automatic vacuum lines attached directly to a Thermo MAT 253 mass spectrometer at Caltech following Passey and others (2010). $\delta^{13}C$ and $\delta^{18}O$[1] values of CO_2 were measured by comparison of samples to a gas with a known isotopic composition using an ion correction algorithm in the Isodat software program (Huntington and others, 2009) and standardized to the VPDB scale for carbon-isotope measurements and VSMOW for oxygen-isotope measurements. Carbonate $\delta^{18}O$ values were calculated from the CO_2 values assuming that the isotopic fractionation factor ($^{18}R_{CaCO3}/^{18}R_{CO2}$) for phosphoric acid digestion at 90 °C is 1.00821 (Swart and others, 1991). We use the same acid digestion fractionation factor for all samples.

Δ_{47} values were standardized by comparison of samples with gases that were heated to 1000 °C in order to achieve a near random distribution of isotopes following Huntington and others (2009), and reported in the 'Ghosh' (or Caltech intralab) reference frame (Ghosh and others, 2006; Dennis and others, 2011). We also provide all Δ_{47} measurements in the absolute reference frame by following Dennis and others (2011) and using standards run in the lab with both known Δ_{47} values in both the Ghosh and absolute reference frames. We analyze and perform all models using data in the Ghosh reference frame because data points used in the Δ_{47} versus temperature calibration (fig. 3) here were universally produced in the Ghosh reference frame at Caltech. Some of the data in this calibration are published (Ghosh and others, 2006; Guo and others, 2009), and have been converted to the absolute reference frame (Dennis and others, 2011), but the dolomite calibration (see below), which ranges from 25 to 350 °C and represents a key temperature interval for high temperature processes, has only been presented in abstract form (Bonifacie and others, 2011) in the Ghosh reference frame. Thus, in order to convert our Δ_{47} values into temperatures in what we believe to be the most self-consistent manner, we keep all data in the Ghosh reference frame.

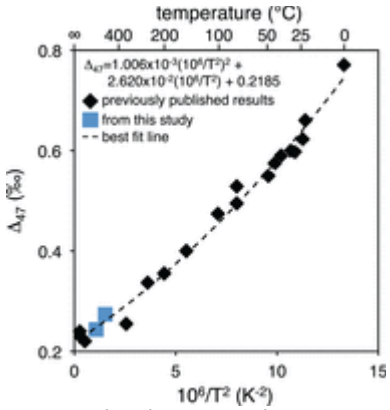

View larger version:

- In this page
- In a new window

Fig. 3.
Data used for the temperature vs. Δ_{47}calibration. All Δ_{47} values are presented in the Ghosh reference frame. Data include experimental measurements on dolomites from Bonifacie and others (2011) and calcites from Ghosh and others (2006), Guo and others (2009) and the work presented here. These temperatures range from 1 to 1650 °C. We note that the non-zero intercept is the result of an 'acid-digestion' fractionation between the released CO_2 isotopologues and the carbonate CO_3 isotopologues. This is discussed in detail both from a theoretical and experimental perspective in Ghosh and others (2006) and Guo and others (2009). The best-fist line is a least-squares regression to the data.

For some analytical sessions the reference frame of measured states of ordering as defined by the gases heated at 1000 °C changed slowly with time (for example, Passey and others, 2010). Δ_{47} measurements of secondary carbonate standards during these sessions demonstrated that an accurate standardization could be accomplished by normalizing data to heated gases analyzed close in time to carbonate samples (generally within a 2-4 day window bracketing the time of sample analysis). Precision and accuracy of Δ_{47} values were determined by measuring a Carrara marble standard multiple times within each measurement session. The average Δ_{47} value in the Ghosh reference frame obtained over the course of 2 years and 49 measurements was 0.360 ± 0.014 permil (1 standard deviation; σ), as compared to long-term average of 0.352 permil.

Calcite heating experiments were conducted on an optical grade calcite (see below) more depleted (that is, lower in δ value) in both carbon and oxygen isotopes ($^{47}\delta$=−34‰[2]) than our secondary standards or commonly analyzed heated gases ($^{47}\delta$∼ −5 to 28‰). In order to standardize the Δ_{47} values of these optical calcites to the heated gas reference frame, additional heated gases more depleted in bulk isotopic composition than the optical calcites were run ($^{47}\delta \cong$ −50‰) to ensure that we were always comparing unknown samples to 1000 °C heated gases with both larger and smaller $^{47}\delta$ values. We noticed that although the external reproducibility of Δ_{47} measurements of optical calcites was normal over the coarse of a session (1σ = 0.014‰), external reproducibly was worse when compared over multiple measurement sessions. To improve external precision across measurement sessions, we performed corrections to the optical-calcite Δ_{47} values using the unheated optical-calcite Δ_{47} values (effectively treating the unheated optical calcite as a secondary standard as in Dennis and others, 2011). In all sessions an unheated optical calcite sample was run daily when heated samples were run (for 33 total measurements of the unheated optical calcite sample). The difference between a given session's average unheated optical-calcite Δ_{47} value from the global average across all sessions was added to all optical-calcite samples for that session. For example, if a session's unheated optical calcite average was higher in Δ_{47} by +0.01 permil than the global average, 0.01 permil was subtracted from all heated optical calcites for that session. Six of the seven sessions had corrections less than 0.024 permil, less than 2σ of our general reproducibility (1σ ≈ 0.014 ‰). One session required a larger correction of 0.037 permil. Similar types of correction have been applied previously, generally due to subtle changes in the heated gas reference frame (for example, Passey and others, 2010). We emphasize this was only done for the optical calcites, and we infer it was necessary only due to the especially low δ_{47} value of CO_2 evolved from that material.

We applied a different kind of empirical correction to the Δ_{47} value of one heated apatite measurement (500 °C, 5.5 hours). This sample was run in a different session from the other apatite samples heated to 500 °C. An unheated sample from Siilinjarvi run directly before this sample was 0.077 permil lower than the average Δ_{47} value measured for unheated Siilinjarvi apatites. We corrected this single apatite sample by adding 0.077 permil to its Δ_{47} value. This correction places the 500 °C, 5.5 hour apatite sample very near a point interpolated between the samples heated for longer and shorter times. Thus, while this correction is large, it appears to have been successfully accounted for. In any event, this data point does not drive any first-order interpretations in this study and, therefore, it could be ignored.

Conversion of Δ_{47} Values to Apparent Equilibrium Temperatures

All Δ_{47} values were converted to apparent equilibrium temperatures by assuming that all carbonate minerals (including apatites) share an identical Δ_{47}versus temperature relationship. To make this conversion, we used experimental data from synthetic calcites precipitated from 1 to 50 °C (Ghosh and others, 2006), dolomites precipitated from 25 to 350 °C (Bonifacie and others, 2011), calcites internally re-equilibrated in the high-temperature cold-seal apparatus experiments described below from 500 to 700 °C, and calcites recrystallized from 1100 to 1650 °C in piston cylinder experiments (Ghosh and others, 2006; Guo and others, 2009) — for such high temperature experiments (that is to say, the piston cylinder experiments), quench effects during cooling are potentially an issue. Specifically, it is possible that Δ_{47} values are modified to higher values at the end of the experiment when the sample is cooled to room temperature due to internal isotope-exchange reactions. Assuming for the highest temperature data from Guo and others (2009) and, as given in that study, linear cooling from 1650 °C to 200 °C within 20 seconds, the paired model presented below predicts the maximum recordable apparent equilibrium temperature for these experimental conditions is 950 °C. The difference in Δ_{47} values of 950 °C (0.237‰) and 1650 °C (0.227‰) is less than the general internal precision of a measurement, so we consider this effect negligible. All data points used to make this calibration are presented in figure 3.

The assumption that calcites and dolomites share an identical temperature vs. Δ_{47} relationship is supported by the theoretical study of Schauble and others (2006) that predicts that the cation and crystal structure of the carbonate containing mineral has a negligible (that is, unmeasurable beyond error) effect on clumping in calcite versus dolomite. This assumption is also supported by the observation that the experimental calcite and dolomite clumped-isotope calibrations overlap (Ghosh and others, 2006; Bonifacie and others, 2011). The assumption that calcite and apatite have identical temperature vs. Δ_{47}relationships is supported by theoretical models at all temperatures and by experiments at low temperatures (24–37 °C; Eagle and others, 2010). High-temperature experiments described below from 500 to 700 °C also support this assumption. Although there is no theoretical prediction regarding the differences in acid digestion fractionation between calcite and carbonate groups in apatite for clumped-isotope measurements, the experimental results of Eagle and others (2010) suggest that any such differences are smaller than the error of the measurement.

Heating Experiments

A series of heating experiments were performed on optical calcites and apatites — the samples used are described in the *Materials* section below. Heating experiments were conducted in a rapid-quench furnace set-up with a René 41 metal cold-seal bomb (Blank and others, 1993). Samples were run between 50 to 65 MPa using argon gas to pressurize the bombs. No water was added to the samples. Bombs were pre-heated to the temperature of interest with the sample held at room temperature in the quenching portion of the bomb. Once the temperature stabilized (though temperatures did sometimes drift by <5 °C, usually down over the course of some experiments) samples were introduced into the hot spot of the bomb by being 'levitated' on a magnetic pedestal. They were heated for a specific time period, which varied for each experiment, and then quenched by dropping the magnet, immediately causing the sample to drop into the cold portion of the bomb (~room temperature) where cooling occurred within 2 to 3 seconds (Ihinger, ms, 1991).

Temperatures in the cold-seal bombs were measured with a type K thermocouple (chromel-alumel) inserted into a drilled hole near the top the bomb. The hole does not penetrate the pressurized interior. We calibrated this outside temperature by measuring an internal temperature gradient along the top three inches of the cold-seal while it was open to air. We report for all experiments the temperature 0.5 inches from the top of the cold-seal, which is the midpoint of our larger capsules. This mid-point temperature is based on a quadratic fit to the measured temperatures vs. the measured distance to the top of the cold-seal (0, 1, 2, and 3 inches). We estimate our error as the maximum temperature difference between 0.5 inches and 0 and 1 inches, which is ±12 °C. For all heating experiments large (mm size or greater) grains were used. Samples were contained in platinum capsules open to the argon atmosphere. Before loading samples, platinum capsules were pre-cleaned in 0.5 M (or greater) HCl for an hour, sonicated in acetone for 5 minutes, then heated at 1000 °C for ten minutes in a 1 atm furnace.

Acid Washing Experiments

Acid cleaning experiments were conducted in 0.1 M acetic acid adjusted to a pH of 4.5 on crushed apatite samples from Siilinjarvi and Oka following Eagle and others (2010). ~1 gram of sample was immersed in the acetic acid for 4 or 24 hours, shaken occasionally, then washed three times with deionized H_2O and dried overnight between 70 to 90 °C.

Fitting of Models to Experimental Data

For fits of models to the experimental data, the trust-region nonlinear least squares fitting algorithm of Matlab was used to find the best fit. Robust fitting was used with the bisquare option. All equations fit to the data are ordinary differential equations. These ordinary differential equations are integrated during the fitting algorithm using Matlab's ordinary differential equation solver ODE45.

Trace Element Compositions of Optical Calcites

The trace element composition (FeO, MgO, and MnO) of the optical calcite used in the experiments was measured on a JEOL JXA-8200 electron microprobe micro-analyzer at Caltech. Chips of the optical calcite were embedded in epoxy and polished. A 100 nA current was used with a spot size of 80 μm. Detection limits were ~0.01 weight percent. 11 different spots were analyzed to check for heterogeneity in the sample.

MATERIALS

Carbonatites

$\delta^{13}C$, $\delta^{18}O$, and Δ_{47} values were measured on carbonate minerals and apatites from three different calcitic carbonatite intrusions (table 1): Kovdor (Russia, 370 Ma), Oka (Canada, 160 Ma), and Siilinjarvi (Finland, 2600 Ma), where Ma signifies the intrusion age in millions of years ago (Nadeau and others, 1999). These intrusions are estimated to have been emplaced at depths of 1 to 3 km for Oka, 3 to 7 km for Kovdor, and 7 to 10 km for Siilinjarvi (Kapustin, 1986). The Oka and Siilinjarvi samples and apatites from Kovdor examined here are splits of the same samples analyzed in the study of Nadeau and others (1999); the Kovdor carbonate samples were provided by Keith Bell (Carleton University). Although all samples come from calcitic carbonatites (Kapustin, 1986; Nadeau and others, 1999), calcite samples can contain trace dolomite, siderite, or magnesite (for example, Haynes and others, 2002). Thus, following Nadeau and others (1999) and Dennis and Schrag (2010), we refer to these samples (excluding apatite samples) in the most general sense as carbonates. All apatite samples are fluroapatites and contain between 0.3 to 2.2 weight percent CO_2 (all compositional data of apatites comes from Nadeau and others, 1999, and are provided in table 1). Apatite samples from Kovdor and Siilinjarvi were reported by Nadeau and others (1999) to contain neither fluid nor carbonate inclusions, but Oka was reported to contain both (table 1). Samples are from carbonatites as opposed to associated fenites (Nadeau and others, 1999).

View this table:

- In this window

- In a new window

Table 1

Ages, inclusions, chemical compositions, isotopic values, and apparent equilibrium temperatures of carbonatite samples

Heating Experiments

Heating experiments were performed on optical calcites from Mexico and apatite from the Siilinjarvi carbonatite (see above). The optical calcite crystals were obtained from the Caltech mineral research collection, but their source within Mexico is unknown. The optical calcite was subsampled for all experiments by chipping material from the crystal along cleavage planes. For apatite heating experiments, subsamples were chipped from a larger crystal.

The optical calcite was measured for MgO, FeO, and MnO weight percents. MgO and FeO were both found to be below detection limits (~0.01 wt. %). MnO was found to be, on average, 0.064 ± 0.004 weight percent (1 standard error; s.e.). The MnO content appeared homogenous in the crystals analyzed — the detection limit, 0.012 weight percent, was similar to the standard deviation of all measurements, 0.014 weight percent.

For apatites, each experimental run product could only be analyzed once as the platinum capsule could at most contain 250 mg of sample (the minimum amount needed for an isotopic measurement of Siilinjarvi apatite). Experimental run products of optical calcites, on the other hand could be analyzed in replicate. For the experiment in which apatite was heated for 5.5 hours at 536 °C and all experiments in which apatite was heated to 692 °C, two different 250 mg aliquots of sample were subjected to experimental heating and then combined and measured as a single sample.

Our first heating experiments yielded results at odds with the rest of our observations: optical calcites were heated at 536 °C for 1 hour, 24 hours, and 72 hours, and yielded run products with Δ_{47} values of 0.545, 0.356 and 0.402 permil respectively. These results lack the evidence for rapid changes in Δ_{47}during the first hour of heating seen in later experiments. Additionally, this is the only case in which a relatively long heating experiment results in a significantly higher Δ_{47} than shorter heating experiments at the same temperature. We noticed nothing unusual about either the experimental procedures or the measurements of run products for these experiments, but suspect that an unnoticed error or irregularity in procedure occurred in this first attempt. For this reason, and because of the peculiar nature of the resulting data, we do not consider these experiments in our general interpretation described below and do not include them in the data tables.

RESULTS AND DISCUSSION

Carbonatites

The measured stable-isotope compositions (including clumped-isotope compositions) of carbonates and cogenetic apatites from the three carbonatites are given in table 1. $\delta^{13}C$ values range from −3.6 to −5.3 permil with similar values for apatite and carbonates in the Oka and Siilinjarvi samples. In the Kovdor samples, the $\delta^{13}C$ value of the carbonate is lower by ~0.7 permil than the carbonate groups in apatite. $\delta^{18}O$ values of carbonates range from 7.3 to 8.3 permil and 8.2 to 11.0 permil for apatites. In all cases, carbonates have lower $\delta^{18}O$ values than cogenetic apatites. Δ_{47} values range from 0.361 to 0.423 permil for carbonates and 0.415 to 0.532 permil for apatites. A key first-order result of these measurements is that in all cases carbonate groups in apatites record higher Δ_{47} values than coexisting carbonates.

The carbonatite Δ_{47} values yield apparent equilibrium temperatures of ~125 to 190 °C for carbonates and ~60 to 130 °C for apatites (table 1 and fig. 4). For Siilinjarvi, two different apatite samples were measured giving 83 ± 2 and 62 ± 1 °C (1 s.e.). We do not know the cause of this difference but it implies some unknown heterogeneity within the carbonatite. The carbonate-mineral apparent equilibrium temperatures are similar to those observed for slowly cooled calcitic marbles (150–200 °C; Bonifacie and others, 2013, Ghosh and others, 2006) as well as other intrusive carbonatites (~100–300 °C; Dennis and Schrag, 2010). Interestingly, for all three

carbonatites, the apatites yield apparent equilibrium temperatures ~40 to 60 °C lower than cogenetic calcites. A simple interpretation of this difference is that carbonate groups in apatite have a lower apparent equilibrium blocking temperature than carbonate minerals.

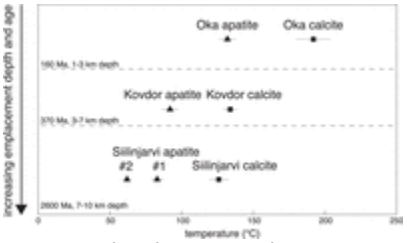

View larger version:

- In this page
- In a new window

Fig. 4.
Apparent equilibrium temperatures from calcites and apatites from carbonatites. Ages are from Nadeau and others (1999). Emplacement depths are from Kapustin (1986). Error bars are 2 standard errors. Ma signifies millions of years ago. Apatites give lower temperatures than calcites in all cases implying they have a lower apparent equilibrium blocking temperature.

It is possible that our results for carbonate groups in apatite reflect contamination by other carbonate bearing minerals. We measured up to 500 mg of apatite, releasing an amount of CO_2 equivalent to that released from ~8 mg of calcite. Additionally, apatites from Oka have been documented to contain carbonate inclusions (table 1; Nadeau and others, 1999). Consequently, even a fraction of a percent of calcite contamination in our apatite samples could influence our results. We explored this issue by cleaning apatite samples in acetic acid prior to stable isotope analyses (see *Methods* section). Dilute acetic acid dissolves so-called labile carbonate groups and calcite but is not believed to attack structural carbonate groups in apatites (Koch and others, 1997; Kohn and Cerling, 2002; Eagle and others, 2010). Apatites from Siilinjarvi were treated for 4 and 24 hours and those from Oka for 4 hours. In no cases did we observe a statistically significant shift in Δ_{47} between treated and untreated apatite samples (table 2). We conclude that trace contamination from calcite and other forms of labile carbonate groups does not contribute sufficient CO_2 to influence our results. Consequently, throughout the rest of this paper, we do not differentiate between acetic-acid-treated and untreated apatite samples.

View this table:

- In this window
- In a new window

Table 2

Cleaning experiment of Siilinjarvi and Oka apatites using acetic acid (see Methods)

An additional source of contaminant CO_2 in the samples could be CO_2 trapped in fluid inclusions and released during mineral digestion in phosphoric acid. This CO_2, if it equilibrated isotopically within the fluid inclusion at laboratory temperatures (for example, ~25 °C), would have elevated Δ_{47} values (~1‰; Wang and others, 2004). Only the Oka apatite sample has been documented to contain fluid inclusions (table 1; Nadeau and others, 1999). However, the Oka apatite samples yielded the highest (hottest) apparent equilibrium temperatures as compared to the Siilinjarvi and Kovdor samples. This is the opposite of what would be expected if fluid inclusions strongly influence a sample's clumped-isotope composition. Although this does not demonstrate that the fluid inclusions have not influenced the results from the Oka apatites, it indicates that dissolved CO_2 is unlikely to be responsible for the variations in Δ_{47} that guide our discussion below.

Igneous crystallization temperatures are demonstrably not recorded by the measured apparent equilibrium temperatures because crystallization of carbonatite melts occur at temperatures around 650 °C (Wyllie and Tuttle, 1960), while all measured apparent equilibrium temperatures are less than 200 °C. This indicates that the apparent

equilibrium temperatures recorded by both the apatites and carbonates in carbonatites record and reflect post-formational processes — this result for carbonates is the same as that found previously by Dennis and Schrag (2010). A relevant question is whether or not the measured Δ_{47} values reflect the kinetics of isotope-exchange reactions or recrystallization during cooling or later metamorphism/diagenesis. Recrystallization is of concern because carbonate minerals in carbonatites commonly recrystallize, often rapidly, after crystallization (Zhabin, 1971). Such recrystallization is documented to have occurred in samples from Siilinjarvi (Tichomirowa and others, 2006) and has likely occurred in all samples. However, much of this recrystallization occurs at elevated temperatures close to the time of original crystallization (Zhabin, 1971). Thus, it is possible that this recrystallization occurs above the nominal apparent equilibrium blocking temperature of the carbonate and allows for internal isotope-exchange reactions to continue during further cooling. If so, it has no impact on the final apparent equilibrium temperatures recorded by a slowly cooled carbonatite.

Several observations lead us to argue that the measured apparent equilibrium temperatures are largely or entirely controlled by isotope-exchange reactions within the mineral lattice as opposed to recrystallization during original cooling or later possible diagenesis/metamorphism. First, apatites are thought to be more resistant to recrystallization in carbonatites than carbonate minerals (Zhabin, 1971), yet we find apatites yield consistently lower apparent equilibrium temperatures (40–60 °C lower) than co-genetic carbonates (table 1 and fig. 3).

Second, the carbonate minerals in our samples show no obvious signs of later diagenesis in their carbon and oxygen-isotope ratios. All carbonate-mineral oxygen-isotope compositions fall within the field defined by Taylor and others (1967) for 'primary' carbonatites (~6–8.75 ‰ relative to VSMOW). Taylor and others, (1967) additionally defined a pristine carbon-isotope field between −5 to −8 permil. Siilinjarvi and Kovdor ($\delta^{13}C$ = −3.65 and −4.02‰, respectively) differ from this field, but plausibly for reasons unrelated to diagenesis. For example, Siilinjarvi's higher carbon-isotope ratio compared to the field of Taylor and others (1967) was argued by Tichomirowa and others (2006) to be the result of magmatic fractionations during differentiation of the parent melt of the carbonatite. No such explanation has been offered for Kovdor's elevated carbon-isotope ratio. However, because oxygen isotopes tend to be more reliable indicators of open-system exchange in carbonates than carbon isotopes (for example, Banner and Hanson, 1990), we consider Kovdor's oxygen-isotope composition to be a sufficient argument for its lack of significant diagenesis.

Third and finally, the differences in carbonate apparent equilibrium temperatures between the intrusions examined here are consistent (at least in direction) with the expected effects of gradual slowing of internal isotope-exchange reactions during cooling of igneous bodies. Oka gives the highest apparent equilibrium temperatures, Kovdor is intermediate and Siilinjarvi is the lowest in temperature for each phase. Importantly, this ranking applies to both calcite and apatite. These temperature trends correlate to emplacement depths (fig. 4): Oka is estimated to have been emplaced the shallowest (1–3 km), Kovdor is intermediate (3–7 km) and Siilinjarvi is the deepest (7–10 km; Kapustin, 1986). More deeply intruded magmas are generally expected to cool more slowly as compared to more shallowly emplaced intrusions because of higher ambient temperatures at the depth of emplacement. Because apparent equilibrium blocking temperatures generally decrease with decreasing cooling rate (Zhang, 2008), we should expect Oka to have cooled the fastest and record the highest apparent equilibrium temperatures, for Kovdor to have cooled more slowly and record a lower temperature, and for Siilinjarvi to have cooled slowest and preserve the lowest temperatures. This prediction is met by the measured temperatures. We thus consider that the apparent equilibrium temperatures recorded in carbonatite carbonate minerals and apatites measured here most likely reflect apparent equilibrium blocking temperatures and not crystallization or recrystallization temperatures.

Heating Experiments

Clumped-isotope measurements from originally high-temperature natural samples provide an important window into processes like solid-state internal isotope-exchange reactions that occur over geologic timescales. However, the thermal histories of natural samples are rarely known precisely and may include multiple episodes of heating, cooling and reaction (or other complexities), limiting their use in making quantitative predictions. Laboratory heating experiments, on the other hand, allow for controlled changes in Δ_{47} values and thus quantitative evaluations

of the kinetic rate constants of interest. The disadvantage of laboratory experiments is that, in general, they must be performed at temperatures higher than observed in natural environments of greatest interest in order to generate measurable changes on laboratory time scales. Such a strategy inevitably requires extrapolation of high-temperature-derived experimental data to lower temperature natural environments, which may or may not be justified. Regardless, if the kinetics of internal isotope-exchange reactions within carbonate-bearing minerals can be well understood via laboratory manipulations and critically examined and justified through comparison to samples with known or well-constrained thermal histories, then these kinetics can be used to answer geologically relevant questions.

The results of analyses of products of our heating experiments (see *Methods*) can be found in table 3 for calcites and table 4 for apatites. The measurement of unheated Siilinjarvi apatite (that is, the initial time point in the plots and tables) is the average of two measurements on Siilinjarvi samples taken from the same batch of apatites used for the experiments. Because apatites from Siilinjarvi vary in starting Δ_{47} (table 1), the products of heating experiments must be compared with the initial composition of these two sub-samples of the starting materials rather than other Siilinjarvi samples.

View this table:

- In this window
- In a new window

Table 3

Bulk and clumped-isotope data and temperatures from heating experiments on calcites

View this table:

- In this window
- In a new window

Table 4

Bulk and clumped-isotope data and temperatures from heating experiments on apatites from Siilinjarvi

Some general observations can be made about the heating experiments for both calcites and apatites. Δ_{47} values of calcite samples held at 209 °C for 7 days and 323 °C for 6 days and apatite samples held at 430 °C (fig. 6A) from 1 hour to 1 day do not change, beyond measurement error (±2 s.e.), from their initial Δ_{47}values. This is consistent with results from Passey and Henkes (2012) for calcites. In all other experiments, Δ_{47} values decrease monotonically with time (figs. 5 and 6). Also, importantly, rates of change of Δ_{47} values increase with increasing temperatures — the 430 °C calcite experiments change in clumped-isotope composition the slowest, never reaching a stable value (fig. 5A), while the 692 °C calcite experiments stabilize in minutes (fig. 5C). The 536 °C calcite experiments stabilize in clumped-isotope composition over the course of hours (fig. 5B.). This is the expected relationship for reaction rates, which generally follow Arrhenian rate laws (see *Extrapolation of Kinetic Properties to Other Temperatures* section below). An interesting observation of the 430 °C experiments is that the data has a distinctively ‘kinked’ shape to its evolution in Δ_{47} with time as opposed to a smooth decrease in Δ_{47} with time (fig 5B). These kinks appear to be a universal feature of these types of experiments, appearing in other optical calcites (fig. 5D; Passey and Henkes, 2012), void-filling spar (Passey and Henkes, 2012), and brachiopod shells (Henkes and others, 2014). We return to the importance of these kinked features when models are constructed to quantify the experiments below.

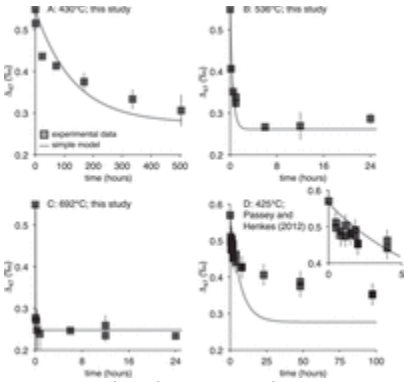

View larger version:

- In this page
- In a new window

Fig. 5.
Simple, pseudo-first-order model as applied to optical-calcite data from calcite heating experiments performed in this study and an example as applied to measurements from Passey and Henkes (2012). (A) 430 °C data; (B) 536 °C data; (C) 692 °C data; (D) Optical-calcite 425 °C data from Passey and Henkes (2012). The inset shows data between 0 and 5 hours. All Δ_{47} values are presented in the Ghosh reference frame. Error bars are 2 standard errors. This simple model in unable to fit the 430 °C data measured in this study nor that measured in Passey and Henkes (2012) or Henkes and others (2014).

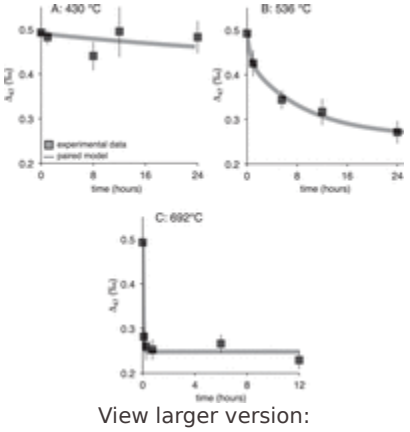

View larger version:

- In this page
- In a new window

Fig. 6.
Paired model as applied to apatite data from apatite heating experiments. (A) Extrapolation of diffusion and exchange parameters derived from the 536 and 692 °C data as applied to the 430 °C data; (B) 536 °C data; (C) 692 °C data. All Δ_{47} values are presented in the Ghosh reference frame. Error bars are 2 standard errors.

Our 430 °C experiments do not reach a constant value of Δ_{47} indicating that internal isotopic equilibrium was never reached (figs. 5A and 6A). The 536 °C and 692 °C calcite (figs. 5B and 5C) and apatites (figs. 6B and 6C), on the other hand do reach constant Δ_{47} values, within the error of measurements, at the end of each experiment. We interpret the constant Δ_{47} values reached at the end of the 536 °C and 692 °C experiments for both apatites and calcites to represent equilibrium Δ_{47} values at those temperatures. The final Δ_{47} value for the 536 °C calcite experiments (using the final 3 time points) is 0.274 ± 0.007 permil (1 s.e.) and 0.244 ± 0.004 permil (1 s.e.) for the 692 °C calcite experiments (using the final 5 time points). In comparison, the final values in the apatite experiments are 0.271 ± 0.013 permil (1σ) at 536 °C (using the final time point) and 0.252 ± 0.008 permil (1 s.e.) at 692 °C (using the final four time points). Significantly, within error, apatites and calcites equilibrated at high temperature

have the same Δ_{47} values. This result is consistent with the model predictions of Eagle and others (2010), and supports our assumption that at equilibrium carbonate groups in calcite and apatite have the same Δ_{47} values.
The 536 °C and 692 °C equilibrium Δ_{47} values calculated above are also consistent with previous experimental calibrations of the carbonate clumped-isotope thermometer at high temperature, with values between the >1100 °C piston cylinder experiments (Ghosh and others, 2006; Guo and others, 2009) and 25 to 350 °C dolomite experiments (Bonifacie and others, 2011) (fig. 3).

MODELING THE EXPERIMENTAL DATA

We present a kinetic model as an aid to understanding and quantifying the experimental heating results of the previous section. Any such model should incorporate both the observed increase in overall reaction rate with temperature and, ideally, be able to fit the two-phased time evolution ('kinks') of the exchange process observed in our 430 °C calcite experiment and those of Passey and Henkes (2012) and Henkes and others (2014).

We present two separate models that attempt to quantitatively explain these data. Both can explain the increase in the rate of change of Δ_{47} values with increasing temperature, but the first, simpler model fails to model the 'kinks', while the second, more complex model does. We present the simpler model first despite its failure to fully fit our experimental results because its discussion illustrates the essential features of the kinetics of changes in Δ_{47} values of carbonates during heating. The derivation of the simple model is similar to that found for clumped-isotope reactions in Appendix A of Passey and Henkes (2012), and for other sorts of reactions in Zhang and others (1995). Following this section, we develop and apply a more complex model that explains all major features of the data using an approach that is inspired by the work of Zhang and others (1995).

'Simple' Model

Changes to the Δ_{47} values of our experimental run products are likely controlled by both exchange reactions in which isotopes are swapped between different carbonate groups and by the rate of short-range diffusion of those different isotopes in the crystal lattice. Modeling of diffusion in our experiments is challenging because there is no length scale inherent to the measurement. In general, diffusivities are measured either by introducing a tracer on a surface or via exchange of a tracer between phases (Cherniak and others, 2010). This kind of information is not generated by our experiments. To deal with this, our 'simple' model implicitly assumes that isotopic diffusion in solid carbonates occurs sufficiently rapidly that it is not the rate-limiting step (Zhang and others, 1995). We note that it can be shown that the mathematics of diffusion for these reactions can mimic the kinetics of isotope-exchange reactions (Appendix 1 of Passey and Henkes, 2012). The kinetics of isotope-exchange reactions between already adjacent carbonate groups controls the reaction rate according to the follow equation:

$$^{12}C^{16}O_3^{2-} + {}^{13}C^{16}O_2{}^{18}O^{2-} \leftrightarrow {}^{12}C^{16}O_2{}^{18}O^{2-} + {}^{13}C^{16}O_3^{2-}. \quad (3)$$

The excess of $^{13}C^{16}O_2{}^{18}O^{2-}$ relative to a random distribution of isotopes that should be present when this reaction reaches equilibrium can be described by a Δ_{63} value with a form similar to equation (2). Specifically, $\Delta_{63} = 1000 \times [(^{63}R/^{63}R^*-1)-(^{62}R/^{62}R^*-1) - (^{61}R/^{61}R^*-1]$, where ^iR is the ratio of the concentration of all mass i isotopologues relative to the concentration of $^{12}C^{16}O_3$ and * refers to a system identical in bulk isotopic composition to the material of interest, but where all isotopes are randomly distributed amongst all isotopologues. We make a further approximation at this point: although there are multiple carbonate species that contribute to the Δ_{47} value of CO_2 extracted from carbonates ($^{12}C^{17}O^{18}O_2{}^{2-}$, $^{12}C^{17}O_2{}^{18}O^{2-}$, $^{12}C^{16}O^{17}O^{18}O^{2-}$, $^{13}C^{16}O_2{}^{18}O^{2-}$, $^{13}C^{16}O^{17}O_2{}^{2-}$, $^{13}C^{17}O_2{}^{18}O^{2-}$, $^{13}C^{17}O_3{}^{2-}$, $^{13}C^{16}O^{17}O^{18}O^{2-}$, $^{13}C^{16}O^{18}O_2{}^{2-}$) the $^{13}C^{16}O_2{}^{18}O^{2-}$ group contributes ~97 percent of the total signal of mass 47 CO_2 isotopologues measured via mass spectrometry. Inclusion of all the species would introduce more free variables than we are currently able to constrain. As such, we proceed here and in the model following to assume that Δ_{47} values are controlled by equation (3). Additionally, we assume that the Δ_{63} of a sample is directly related to the Δ_{47} of CO_2 extracted from that carbonate by acid digestion through the expression: $\Delta_{47} = \Delta_{63} + 0.219 \pm 0.010‰$ (1σ), which is the extrapolated intercept in figure 3. This intercept represents the isotopic fractionation

associated with conversion of CO_3 groups to CO_2 for analysis. Guo and others (2009) present an argument that the offset associated with acid digestion could be a subtle function of Δ_{63} rather than a constant; however, no published experimental evidence supports this more complex treatment of the acid digestion fractionation. As such we assume that the offset between Δ_{63} and Δ_{47} is constant.

We first assume that equation (3) is elementary (reacts as written and not through unspecified intermediates). Additionally we write all reactions in terms of a reaction progress parameter, ξ (Zhang, 2008), which tracks the change in the number of $^{13}C^{16}O_2{}^{18}O^{2-}$ molecules with time. At the start of each experiment ξ is zero as no $^{13}C^{16}O_2{}^{18}O^{2-}$ molecules have been generated or consumed until the experiment begins. Using ξ we write

$$\frac{d\xi}{dt} = k_f[^{12}C^{16}O_3{}^{2-}][^{13}C^{16}O_2{}^{18}O^{2-}] - k_b[^{12}C^{16}O_2{}^{18}O^{2-}][^{13}C^{16}O_3{}^{2-}]. \quad (4)$$

The k_f and k_b are the forward and reverse reaction constants respectively. [x] represents the concentrations of the species normalized such that the total of all carbonate isotopologues is equal to one. At equilibrium, by definition, the forward and reverse reaction rates balance:

$$k_f[^{12}C^{16}O_3{}^{2-}]_{eq}[^{13}C^{16}O_2{}^{18}O^{2-}]_{eq} = k_b[^{12}C^{16}O_2{}^{18}O^{2-}]_{eq}[^{13}C^{16}O_3{}^{2-}]_{eq} \quad (5)$$

where the $[x]_{eq}$ represents the concentration of a given isotopologue at equilibrium. We can rewrite this reaction in terms of the equilibrium constant:

$$\frac{k_f}{k_b} = \frac{[^{12}C^{16}O_2{}^{18}O^{2-}]_{eq}[^{13}C^{16}O_3{}^{2-}]_{eq}}{[^{12}C^{16}O_3{}^{2-}]_{eq}[^{13}C^{16}O_2{}^{18}O^{2-}]_{eq}} = K_{eq} \quad (6a)$$

where K_{eq} is the equilibrium constant for equation (8a). As K_{eq}, which is a function of temperature, is known from experiments conducted between 1 to 1650 °C (fig. 3) we can eliminate k_b from the equation by writing the following:

$$k_b = \frac{k_f}{K_{eq}}. \quad (6b)$$

Additionally, by writing our reactions in terms of a progress parameter, we can rewrite equation (4) in terms of ξ and the initial concentrations of the isotopologues:

$$\frac{d\xi}{dt} = k_f([^{12}C^{16}O_3{}^{2-}]_0 - \xi)([^{13}C^{16}O_2{}^{18}O^{2-}]_0 - \xi) - \frac{k_f}{K_{eq}}([^{12}C^{16}O_2{}^{18}O^{2-}]_0 + \xi)([^{13}C^{16}O_3^{2-}]_0 + \xi) \quad (7)$$

where $[x]_0$ represents the initial normalized concentration of an isotopologue. This equation has only one unknown, k_f and can be solved numerically in a straightforward manner (see *Methods*). We neglect changes in the concentration of all isotopologues except $^{13}C^{16}O_2{}^{18}O^{2-}$ for computational ease. This assumption is actually required because we assume that the bulk $\delta^{18}O$ and $\delta^{13}C$ value of the calcite are constant (see below), which requires that the concentrations of $^{12}C^{16}O_2{}^{18}O^{2-}$ and $^{13}C^{16}O_3{}^{2-}$ are constant as well. This is a reasonable simplification because in a closed system large changes in the abundance of $^{13}C^{16}O_2{}^{18}O^{2-}$ are required to make detectable changes in $^{13}C^{16}O_3{}^{2-}$ or $^{12}C^{16}O_2{}^{18}O^{2-}$. For example, a change in Δ_{47} of ~1 permil creates a change in $\delta^{18}O$ of <0.01 permil, which is well below the external precision of $\delta^{18}O$ measurements (typically ~0.1‰). With a knowledge of $\xi(t)$ we can find the concentration of $^{13}C^{16}O_2{}^{18}O^{2-}$ at any time ($[^{13}C^{16}O_2{}^{18}O^{2-}]_t = [^{13}C^{16}O_2{}^{18}O^{2-}]_0 \pm \xi(t)$), which in turn allows for a calculation of Δ_{63}. Given known bulk isotopic compositions and Δ_{47} values of our experimental run products, we can calculate the normalized concentrations of all the isotopic species in equation (7) following Huntington

and others (2009). Finally, the equilibrium constant at a given temperature is derived from the data of figure 3via the relation: $-1000\ln(K_{eq}) = \Delta_{63}$ (Wang and others, 2004).

An examination of the data in table 3 shows that after heating the optical calcites have a tight distribution of $\delta^{18}O$ (10.1 ± 0.1‰ [1σ]), which is similar to the external precision of the measurement (0.08 to 0.1‰; 1σ). $\delta^{13}C$ values have a larger range (−28.9 to −32‰) that is an order of magnitude larger than the external precision of the measurement (0.025 to 0.04‰; 1σ). There is no correlation between $\delta^{13}C$ and temperature or duration of heating, and the range is similar to that for the optical calcites prior to heating (−29.6 to −32.1‰). We conclude that the $\delta^{13}C$ of the optical calcite sub-samples used for the experiments varies due to heterogeneities in the starting material. Regardless, this isotopic variability has an impact on the modeling as an increase or decrease in the overall bulk $\delta^{13}C$ value changes the overall concentration of $^{13}C^{16}O_2{}^{18}O^{2-}$ for identical Δ_{63} values. As we fit our model to overall concentrations and then convert to Δ_{47} values, differences in bulk isotopic compositions due to heterogeneities in the optical calcite result in each experiment having a different initial concentration of $^{13}C^{16}O_2{}^{18}O^{2-}$. To deal with this, we simplify the problem by using the average $\delta^{13}C$ and $\delta^{18}O$ of our unheated optical calcite as the starting andending bulk isotopic composition for all experiments. However, there may be some circumstances, such as open-system isotope-exchange reactions, where it is important to consider the kinetics of simultaneous changes in clumped-isotope, $\delta^{18}O$ and $\delta^{13}C$ values (for example, Affek, 2013; Clog and others, 2015).

All data (that is, Δ_{47} vs. time at each temperature) are fit as functions of k_f as discussed in the methods section. A fit to the data with this model is presented in figure 5A for the 430 °C experiments, 5B for the 536 °C calcite experiments, and 5C for the 692 °C calcite experiments. The fit is robust for the 692 °C data (r^2=0.98). The fit is poorer but perhaps acceptable for the 536 °C data (r^2= 0.90). However, the fit poorly replicates the data for the 430 °C fit (r^2=0.84). Although the correlation coefficients of all experiments are similar, a visual inspection of the fit through the 430 °C experiment demonstrates that it is indeed a poor fit: it is incapable of capturing the rapid movement at the start of the experiment and overshoots the data towards the end of the experiment. The simple model described above cannot replicate the 'kinked' behavior of the 430 °C calcite heating experiment here and from others (fig. 5D; Passey and Henkes, 2012; Henkes and others, 2014). Consequently, as we consider this 'kinked' shape to be a robust result, in the next section we develop a more complex model with the express purpose of fitting these kinks.

Paired, 'Reaction-Diffusion' Model

In this section we develop a model that can fit the kinked time-dependent changes in Δ_{47} observed in the 430 °C experiments shown here, as well as similar data from Passey and Henkes (2012) and Henkes and others (2014). As discussed above, Passey and Henkes (2012) proposed that the relatively rapid kinetics at the start of the experiments are driven by defects that allow for rapid migration of atoms in the crystal lattice. Because these enhanced kinetics of isotope exchange are only present at the start of the experiment, Passey and Henkes (2012) proposed these defects are annealed out of the calcite early in the course of the experiment. The loss of these fast pathways for isotope exchange causes reaction rates to slow down, generating the kink in the time evolution of Δ_{47} values. This is a plausible explanation because previous studies have shown that annealing of calcites can change the diffusivity of oxygen presumably through an alteration of structural defects (Anderson, 1969; Kronenberg and others, 1984; Farver, 1994). Henkes and others (2014) developed a quantitative model to describe the changes in Δ_{47} values during heating that included a dependence on the rate of defect annealing. However, they concluded that the inclusion of defects in the model versus treating the change in Δ_{47} as a pseudo-first-order problem (similar to the simple model presented above) by only using data in the experiments after the kink only mattered for geologically relevant thermal histories once temperatures reached ~150 °C. Furthermore, because the defects are annealed out of high-temperature systems, they were concluded to be unimportant during cooling histories of igneous and metamorphic rocks (Passey and Henkes, 2012).

It is also worth noting that the optical calcite of Passey and Henkes (2012) and brachiopod of Henkes and others (2014) yielded essentially identical kinetics. If the defect model is correct, this then requires that multiple calcites of different origin have similar defect concentrations. The spar calcite of Passey and Henkes (2012),

on the other hand, yielded far more rapid and complex exchange kinetics than the optical calcite and brachiopod. This complexity required the sample to be modeled as having both a period of defect annealing at the start of the experiment and the presence of two distinct, non-interacting components within the spar with different kinetics for closed-system isotope-exchange reactions. The different style of kinetics for the spar calcite was suggested to be due to a higher concentration of trace metals such as Mn (Passey and Henkes, 2012; Henkes and others, 2014). Additionally, the need to have two non-interacting components with different kinetics in the lattice was supported by the observation that the Mg and Mn contents are heterogeneously distributed in the mineral at the micron scale. We note that our optical calcite is 0.064 weight percent MnO, and thus intermediate in MnO composition between the optical calcite measured by Passey and Henkes (2012; <0.025 wt. %) and those measured by Farver (1994) between 0.01 to 0.15 weight percent. Farver (1994)observed that the diffusivity of O in the sample that is more enriched in Mn was higher by multiple orders of magnitude than the sample that is lower in Mn if samples were not initially preannealed for experiments at 550 °C but not for experiments above 600 °C (that is, the two samples yielded, within error, identical diffusivities above 600 °C). Interestingly, our optical calcite shows identical (within error) kinetic parameters as those of Passey and Henkes (2012), despite being 2 to 3x more enriched in Mn. Thus it is not clear whether differences in Mn or other trace elements, in and of themselves, are sufficient to cause differences in the rate of change of Δ_{47} values during heating.

Here, we take an alternative approach that describes the kinked behavior of clumped-isotope kinetics through an atomistic mechanism that is common to all carbonates, physically justifiable, and capable of mathematically fitting the kinks in the data. Our approach is motivated by the observation that the fast initial reaction rates are present (and appear more or less similar in form) in multiple samples of calcites with a range of heating temperatures and durations studied in two different labs. This can only be true if the factors controlling the rapid kinetics seen early in heating experiments are universal (or at least common). Previous experiments on oxygen self-diffusion in calcites suggest this is unlikely if the factors controlling reaction rate are driven entirely by defects of some kind: Farver (1994), for example, noticed that one of two samples investigated showed a simple Arrhenian dependence of oxygen self-diffusion on the experimental temperature (400–800 °C), while the other sample showed non-Arrhenian behavior. This non-Arrhenian behavior was hypothesized to be caused by the presence of defects. Indeed, this latter sample actually increased in oxygen diffusivity from 600 °C to 550 °C, which is potentially related to more rapid diffusion of oxygen via defects at 550 °C that were rapidly annealed out of the crystal at 600 °C. This suggests that defects could cause increased rates at lower temperatures relative to higher temperature experiments, which is not consistent with either our study of clumped-isotope kinetics or with Passey and Henkes (2012) and Henkes and others (2014).

To account for the kinks in the time dependence of Δ_{47} values in our experimental data, we constructed a more physically complex reaction model inspired by the study of Zhang and others (1995). Our model explains the kinks as a natural consequence of the combined kinetics of diffusion and reaction between rare isotopologues in the carbonate lattice (fig. 7). We describe these combined kinetics by modifying the model of Zhang and others (1995), which was used to model the kinetics of the reaction: $H_2O + O <--> 2OH$ in silicates, where 'O' is an oxygen bound to the silicate lattice.

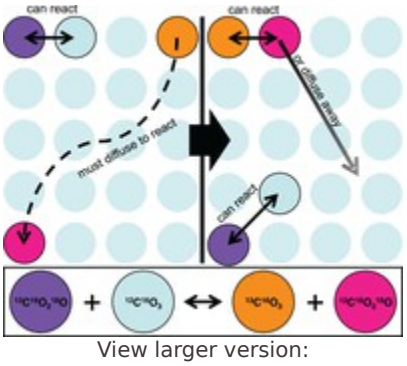

View larger version:

- In this page
- In a new window

Fig. 7.
Cartoon representation of the paired 'reaction-diffusion' model. Most carbonate groups (98%) in the crystal lattice are $^{12}C^{16}O_3$carbonate groups. In this model, $^{13}C^{16}O_2{}^{18}O$ carbonate groups are always found adjacent to $^{12}C^{16}O_3$carbonates. Thus there is no diffusional limitation for these carbonate groups to exchange isotopes. When they exchange isotopes, they form adjacent $^{13}C^{16}O_3$and $^{12}C^{16}O_2{}^{18}O$ groups, which we term 'pairs.' These pairs can either react 'backwards' to reform adjacent $^{13}C^{16}O_2{}^{18}O$ and $^{12}C^{16}O_3$ groups or diffuse apart.
However, $^{13}C^{16}O_3$ and $^{12}C^{16}O_2{}^{18}O$ groups are generally not found (~95% of the time) in a paired configuration but are instead isolated from each other. In order for these groups to exchange isotopes, they must diffuse towards each other until they are in a paired configuration.

The model we present explicitly accounts for the neighbors that surround any chemical species (such as the carbonate ion group) participating in a reaction. The dominant carbonate isotopologue in calcite is $^{12}C^{16}O_3{}^{2-}$ (~98 %). The probability that a carbonate group neighbors at least one unsubstituted carbonate is $1\text{-}0.02^6$, where the 6 is the number of neighboring carbonate groups in a calcite lattice. Consequently, a multiply isotopically substituted carbonate group like $^{13}C^{16}O_2{}^{18}O^{2-}$ can be approximated to always have one or more neighboring $^{12}C^{16}O_3{}^{2-}$ with which it can react to form two singly substituted species. As such, the forward reaction rate of equation (3) is never limited by solid-state diffusion of isotopes through the crystal lattice — the two reaction partners can be approximated to be always present together (fig. 7).

In contrast, exchange of isotopes between the singly substituted carbonate ions $^{13}C^{16}O_3{}^{2-}$ and $^{12}C^{16}O_2{}^{18}O^{2-}$, can be rate limited by solid-state diffusion. For example, $^{12}C^{16}O_2{}^{18}O^{2-}$ groups are 0.6 percent of all carbonate groups and $^{13}C^{16}O_3{}^{2-}$ are 1 percent. Thus, the chance that a given $^{12}C^{16}O_2{}^{18}O^{2-}$ group neighbors a $^{13}C^{16}O_3{}^{2-}$ group for a random distribution of groups in the lattice is 6 percent in a calcite crystal[3]. Consequently, approximately 94 percent of $^{12}C^{16}O_2{}^{18}O^{2-}$ groups in the sample cannot immediately react with $^{13}C^{16}O_3{}^{2-}$to form a clumped species. Instead they can only react to form a clumped species if and when they are adjacent in the lattice (fig. 7).

In this model, we only track the reaction of $^{13}C^{16}O_2{}^{18}O^{2-}$ with $^{12}C^{16}O_3{}^{2-}$ for the removal of isotopologues that can generate CO_2 at mass 47. This is an approximation because reactions between $^{13}C^{16}O_2{}^{18}O^{2-}$ with isotopically substituted species are also possible. However, they need not necessarily result in a net loss of $^{13}C^{16}O_2{}^{18}O^2$. For example, exchange of $^{13}C^{16}O_2{}^{18}O^{2-}$ with $^{13}C^{16}O_3{}^{2-}$ (the dominant isotopically substituted group) consumes one $^{13}C^{16}O_2{}^{18}O^{2-}$ but creates another to replace it. Exchange with a $^{12}C^{16}O_2{}^{18}O^{2-}$or $^{12}C^{17}O^{16}O_2{}^{2-}$ (the next most abundant substituted groups), on the other hand, could generate another multiply substituted species that we are not explicitly modeling due to their low abundance. However, because these two species add up to only ~0.7 percent of carbonate groups in the sample and thus are not common bonding partners, we do not include a correction term for the exchange of $^{13}C^{16}O_2{}^{18}O^{2-}$ with species other than $^{12}C^{16}O_3{}^{2-}$.

Model structure.

We begin by considering the following reactions (see also the illustrative cartoon in fig. 7):

$$^{12}C^{16}O_3^{2-} + {}^{13}C^{16}O_2^{18}O^{2-} \leftrightarrow \text{pair} \quad (8a)_{\text{and}} \quad \text{pair} \leftrightarrow {}^{13}C^{16}O_{3,\,\text{single}}^{2-} + {}^{12}C^{16}O_2^{18}O_{\text{single}}^{2-} \quad (8b)$$

where a pair signifies $^{13}C^{16}O_3{}^{2-}$ and $^{12}C^{16}O_2{}^{18}O^{2-}$ residing next to each other and 'single' signifies a singly isotopically substituted species that does not reside next to another singly isotopically substituted species in the crystal lattice. We term such groups 'singletons'. In this formulation, the pairs represent an intermediary through which clumped species interact with the majority of singly isotopically substituted species. We note that pairs include all situations where there are two or more singly substituted species next to each other including triplets, quadruplets, et cetera (Zhang and others, 1995). Pairs can be formed or destroyed either by diffusion or by reaction.

Model intuition.

The paired model requires that clumped species must first convert to pairs of singly substituted species before finally forming the more common singletons (and vice versa). In this way pairs act as an intermediary between clumped and singly substituted species in the following reaction scheme: clumped species ↔ pairs ↔ singletons. If the concentration of pairs remains constant throughout a reaction (that is, dpair/dt = 0), then they have no effect on the kinetics as any change in the concentration of clumped species will have to, for mass balance considerations, be immediately compensated for by a change in the concentration of singletons. If this were the case, the simple model of the previous section would be reproduced and no kinks would be observed in the time-dependent changes of Δ_{47} values.

If, on the other hand, the concentration of pairs evolves with time, then the pairs can act to modify the kinetics of reactions that form or consume clumped-isotope species. Specifically, if diffusion of the two carbonate ions that make up a pair ($^{13}C^{16}O_3$ and $^{12}C^{16}O_2{}^{16}O_3{}^{2-}$) in the crystal lattice is slow compared to local isotopic exchange between $^{13}C^{16}O_2{}^{18}O^{2-}$ species and $^{12}C^{16}O_3{}^{2-}$ or between the carbonate ions that make up the pairs, the population of pairs will increase or decrease in size (depending on whether clumped species are, in net, forming or being destroyed). In this scenario, the pairs can act as a buffer to changes in the concentration of clumped isotopologues. For example, during heating, as clumped species dissociate to pairs, if diffusion cannot separate the pairs sufficiently quickly, the pair concentration will build to an excess until the back reaction of pairs to clumped species balances the splitting of clumped species to pairs. This would slow and eventually halt the decline in clumped species. As diffusion proceeds and separates the pairs into singletons, clumped species could then continue to react and drop in abundance.

The results of our 430 °C experiment can be understood as the product of this dynamic relationship between singletons, pairs and clumps: the initial fast reaction could occur because there are not enough pairs to buffer the system at the start. Once the pairs are able to buffer the splitting of clumped species, the kinetics become controlled by the slower diffusional separation of pairs to singletons as seen in latter part of the experiment. Thus all of the clumped-isotope experiments showing complex kinetics, both here and in Passey and Henkes (2012) and Henkes and others (2014) can be understood if early in these experiments the initial population of pairs is first driven to a dynamic steady state with the clumped species, after which further reaction requires the slower process of separation of pairs by solid-state diffusion.

Model derivation.

Here, the key equations that are used to fit the data to the paired model are derived following Zhang and others (1995). An equation describing the kinetics of equation (8a), which assumes the reaction proceeds in an elementary fashion, is:

$$\frac{d\xi}{dt} = k_f([^{12}C^{16}O_3^{2-}]_0)([^{13}C^{16}O_2{}^{18}O^{2-}]_0 - \xi) - k_b[\text{pair}]_t. \quad (9)$$

Additionally the concentration of pairs changes as a function of time according to:

$$\frac{d\text{pair}}{dt} = k_f([^{12}C^{16}O_3^{2-}]_0)([^{13}C^{16}O_2{}^{18}O^{2-}]_0 - \xi) - k_b[\text{pair}]_t + k_{\text{dif-single}}[^{12}C^{16}O_2{}^{18}O^{2-}]_{\text{single},0}[^{13}C^{16}O_3^{2-}]_{\text{single},0} - k_{\text{dif-pair}}[\text{pair}]_t. \quad (10)$$

In equation (9) the terms led by the reaction coefficients k_f and k_b represent isotopic exchange reactions and the final two terms led by $k_{\text{dif-single}}$ and $k_{\text{dif-pair}}$represent the process of diffusion and are related to diffusivities (Zhang and others, 1995). Zhang and others (1995) present arguments in support of our description of diffusion in terms of a chemical reaction, guidance for how to envision the length scales inherent to the diffusion problem, and the relationship between the relevant diffusivities of interest and $k_{\text{dif-single}}$ and $k_{\text{dif-pair}}$. We have assumed here that the concentrations of $^{12}C^{16}O_3{}^{2-}$ and the singletons vary so little that they can be treated as constants.

Although equation (10) has four kinetic parameters, they are not all independent. At equilibrium, by definition, $d\xi/dt = 0$. As such we can write,

$$k_f[^{12}C^{16}O_3^{2-}]_{eq}[^{13}C^{16}O_2{}^{18}O^{2-}]_{eq} = k_b[pair]_{eq}. \quad (11)$$

The concentrations of $^{12}C^{16}O_3{}^{2-}$ and $^{13}C^{16}O_2{}^{18}O^{2-}$ at equilibrium are obtained by calculating the expected Δ_{63} at the temperature of the experiment and inverting for the bulk concentrations of the species (as done above in the '*Simple' Model* section).

To find the concentration of pairs at equilibrium we initially assume (following Zhang and others, 1995) that the solid carbonate solution is ideal and thus that at equilibrium the carbonate groups will be randomly distributed in the lattice. We consider this the simplest possible assumption with which to begin, but we discuss below the failure of this assumption and the need to modify it to include a temperature dependence for the number of pairs in the system at internal isotopic equilibrium. We find the number of pairs at equilibrium (presuming for the moment a random distribution of pairs at equilibrium) as follows: we calculate the expected total amount of any given singly substituted carbonate group as was done for the simple model above. If an individual carbonate group is coordinated such that there are Z carbonate groups surrounding it, the number of singleton $^{13}C^{16}O_3{}^{2-}$ groups is: $[^{13}C^{16}O_3{}^{2-}]_{single} = [^{13}C^{16}O_3{}^{2-}]_{total}(1-[^{12}C^{16}O_2{}^{18}O^{2-}]_{total})^z \quad (12a)$ and singleton $^{12}C^{16}O_2{}^{18}O^{-2}$ groups is: $[^{12}C^{16}O_2{}^{18}O^{2-}]_{single} = [^{12}C^{16}O_2{}^{18}O^{2-}]_{total}(1-[^{13}C^{16}O_3^{2-}]_{total})^z. \quad (12b)$

For calcites, we assume a value for Z of 6. Equations (12a and 12b) represent the probability of finding a singleton given a random distribution of isotopologues in the mineral. The concentration of paired species at equilibrium is: $[pair] = [^{12}C^{16}O_2{}^{18}O^{2-}]_{total} - [^{12}C^{16}O_2{}^{18}O^{2-}]_{total}(1-[^{13}C^{16}O_3{}^{2-}]_{total})^z \quad (13a)$ or $[pair] = [^{13}C^{16}O_3{}^{2-}]_{total} - [^{13}C^{16}O_3{}^{2-}]_{total}(1-[^{12}C^{16}O_2{}^{18}O^{2-}]_{total})^z. \quad (13b)$

The concentration of pairs at equilibrium should be independent of whether we choose equation (13a) or (13b). However, as the pairs include situations with two or more singly substituted species next to each other (see above), equations (13a) and (13b) end up differing by 1 percent relative. We average the values of the pairs calculated from equations (13a) and (13b) to find the equilibrium pair distribution. We found that the choice of using equation (13a), (13b), or an average of the two had no noticeable effect on the results. We now write:

$$k_f\frac{[^{12}C^{16}O_3{}^{2-}]_{eq}[^{13}C^{16}O_2{}^{18}O^{2-}]_{eq}}{[pair]_{eq}} = k_b. \quad (14)$$

This allows for the elimination of one free parameter. Another can be eliminated through the requirement of equilibrium for equation (10). At equilibrium, equation (11) holds and the pair concentration is constant. Thus dpair/dt=0 and $k_{dif\text{-}single}[^{12}C^{16}O_2{}^{18}O^{2-}]_{single,eq}[^{13}C^{16}O_3{}^{2-}]_{single,eq} = k_{dif\text{-}pair}[pair]_{eq}, \quad (15a)$ which, if we use our equation for the singletons from above, we can rewrite as $k_{dif\text{-}pair}$

$$= k_{dif\text{-}single}\frac{[^{12}C^{16}O_2{}^{18}O^{2-}]_{eq}(1-[^{13}C^{16}O_3{}^{2-}]_{eq})^z[^{13}C^{16}O_3{}^{2-}]_{eq}(1-[^{12}C^{16}O_2{}^{18}O^{2-}]_{eq})^z}{[pair]_{eq}}. \quad (15b)$$

Now there are only two free parameters, a rate constant for the exchange and a rate constant for diffusion.

Paired model fitting.

We solve for the rate constants, k_f and $k_{dif\text{-}single}$, through a minimization of the solutions of equations (9) and (10) versus the data as discussed in the methods section. These fits require that both ξ and the number of pairs in the system be initialized. ξ is initially set to zero. The correct choice for the initial number of pairs in the system is not obvious, but is important because the concentration of pairs relative to the final equilibrium value at

any given point in time is a critical parameter in the model. We explored how to initialize the pair concentration by generating models in which the initial and final pair concentration values were either identical or different.

We found that initializing the pair concentration to be the same as the proscribed final, randomly distributed pair concentration resulted in a poor fit for the 430 °C calcite experiments and was essentially identical to the fits produced by the simple model in the preceding section (that is, if the pair population does not evolve with time, the kinetics are predicted to be pseudo first order). This demonstrates that differences in the rates of diffusion versus clumped-pair exchange are insufficient on their own to develop large enough temporary excesses or deficits in the concentration of pairs compared to the final value.

In contrast, we observed that model runs where the pairs were initialized with a different concentration than their final, prescribed value did generate kinks. We found that the best fits for the 430 °C experiment occurred if the system was initialized with either a slight deficit of pairs (1% lower) or an enrichment of pairs (0.015% higher) relative to the final value. These values were found by varying the starting pair concentration relative to the value calculated in equation (13), which assumes the probability of finding pairs is random, and searching for the values that provided the best fit as determined by the r^2 value. The final value did not need to be the random concentration pairs — instead only the relative difference between the initial and final number of pairs appears to matter. The need to have a non-random initial concentration of pairs was also required in the modeling of Zhang and others (1995) on which our model is based. In the case of this previous study, no thermodynamic justification for an initial non-random concentration of pairs was given, but was justified as the result of prior thermal histories. Here we hypothesize that excesses or deficits in 'pairs' are not a model artifact but instead arise from a thermodynamic driving force related to the distribution of pairs within a carbonate mineral.

Specifically, we hypothesize that pairs are enriched relative to that expected for a random concentration of pairs throughout the lattice due to a drop in free energy of the system when singly substituted carbonates are found as pairs as opposed to isolated as singletons. Thermodynamically, this requires a non-zero enthalpy of mixing for carbonate groups in the mineral lattice. Although pairs, as we define them, do not involve bonds between two heavy isotopes (which would lower the energy of the system; Wang and others, 2004; Schauble and others, 2006), they still involve a close association of those heavy isotopes. Such associations can be thought of as solid-state versions of clumped-isotope species that lack immediately adjacent heavy isotopes. An example of a molecule that has this property is gaseous $^{12}C^{18}O_2$, where the ^{18}O's are on opposite sides of an isotopically normal (that is unsubstituted) carbon. These 'secondary' clumped species have excesses that are smaller in size, but otherwise generally similar to other clumped-isotope equilibrium reactions (for example, Wang and others, 2004). For example, at equilibrium, $^{12}C^{18}O_2$ is half as enriched as $^{13}C^{16}O^{18}O$ at a given temperature and bulk isotopic composition (Wang and others, 2004). We expect such thermodynamically driven excesses in pairs should be temperature dependent with a stronger favoring of pairs at lower temperatures, and be controlled by equilibrium constants of the form,

$$K_{pair} = \frac{[pair]}{[^{13}C^{16}O_{3,\,single}^{2-}][^{12}C^{16}O_2^{18}O_{single}^{2-}]}, \quad (16)$$

where K_{pair} is the inverse of the equilibrium constant for equation (8b).
No theoretical model for the distribution or size of this hypothesized excess of pairs currently exists — that is, K_{pair} as a function of temperature is not known. We hypothesize that the temperature dependence of K_{pair} follows a relationship in which $\ln(K_{pair})$ is linearly proportional 1/T where T is temperature — this is a common form for the temperature dependence of equilibrium constants for other isotope-exchange reactions (Criss, 1999) and equilibrium constants in general (Denbigh, 1981). This relationship requires that samples formed at lower temperatures will have an excess of pairs compared to a system at a higher temperature and vice versa.
We further assume that the intercept of such a line must be consistent with pairs and singletons being randomly distributed in the lattice at infinite temperatures (that is, entropy is maximized at infinite temperatures), giving an intercept of $\ln(K_{pair,random})$ where $K_{pair,random}$ is the equilibrium constant for the random distribution of pairs and singletons. This too is in keeping with the behaviors of other known isotope-exchange reactions (Criss, 1999) and

chemical systems at equilibrium in general (Denbigh, 1981). Thus, $\ln(K_{pair}/K_{pair,random})$ is linearly proportional to 1/T. The key unknown, therefore, is the slope (that is, the steepness of temperature dependence of pair excess). We assume that our unheated optical calcite formed in internal isotopic equilibrium at its measured apparent equilibrium temperature of 55 °C and has a 0.015 percent excess of pairs compared to equilibrium at 430 °C. This was the excess we found provided the best fit the 430 °C experimental data. We do not use a 1 percent deficit of pairs (which yields an equally good fit) because our model requires samples to have an initial excess of pairs when heated to higher temperatures. As the required excess in pairs has an order of magnitude smaller effect on the concentration of singletons (requiring an ~0.001% drop in the concentration of singletons), we maintain our assumption from above that the singletons do not change in concentration over the course of our experiment. This assumption allows us to approximate $\ln(K_{pair}/K_{pair,random})$ at a given temperature as $\ln([pair]/[pair_{random}]$. Then, solving for the slope by using the known difference in pairs at two different temperatures (55 and 430 °C), we find the following relationship:

$$\ln\left(\frac{[\text{pair}]}{[\text{pair}_{\text{random}}]}\right) = \frac{0.0992}{T} \quad (17)$$

where T is in Kelvin. This relationship allows us to calculate the concentration of pairs at any arbitrary temperature. This treatment of pairs is clearly a hypothesis anchored to an empirical finding of our model fits. However, it is potentially testable through the creation a lattice model that calculates the expected pair excesses as a function of temperature following the work of Schauble and others (2006).

We incorporated equation (17) into our model to find the initial and final pair concentrations and fit the model to the 430, 536, and 692 °C calcite data (fig. 8). The 430 and 536 °C calcite data were straightforward to fit using the methods outlined above due to the large spread in Δ_{47} over the course of the experiments (figs. 8A and 8B; table 5). The 692 °C experiment, on the other hand, is 90 percent equilibrated within 3 minutes (fig. 8C). Because of this, there are few points available to define the curvature. We found that, unlike the 430 and 536 °C cases, different initial guesses for the values of k_f and $k_{dif\text{-}single}$, which are needed to initialize the fitting routine, resulted in different (though generally similar) final answers with indistinguishable goodness of fits — all final fits had r^2 values of ~0.97. This implies that there exist multiple values of k_f and $k_{dif\text{-}single}$ for the 692 °C data that can produce equally robust fits.

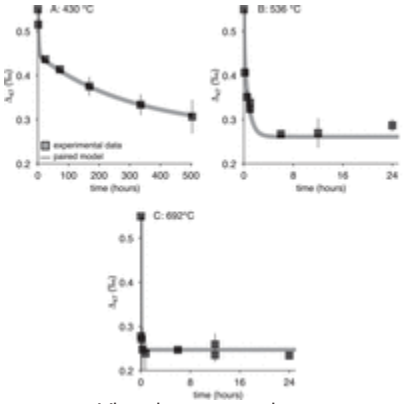

View larger version:

- In this page
- In a new window

Fig. 8.
Paired model as applied to data from optical-calcite heating experiments performed in this lab. (A) 430 °C data; (B) 536 °C data; (C) 692 °C data. All Δ_{47} values are presented in the Ghosh reference frame. Error bars are 2 standard errors.

View this table:

- In this window
- In a new window

Table 5

Rate constants derived from modeling of calcite heating experiments

In order to choose which of these fitted parameters at 692 °C to use in later modeling, we also required that the fits be consistent with our experimental observations that holding the optical calcite for 6 days at 323 °C or 7 days at 209 °C yields no change in Δ_{47} within error of the starting value. In order to test this, we combined all potential 692 °C fitted parameters with those from the 430 and 536 °C fits to create Arrhenian-based models for the temperature dependence of rate constants (see section, *Extrapolation of Kinetic Properties to Other Temperatures*, below) and calculated kinetic parameters for diffusion and exchange at 209 and 323 °C. We then used these parameters to calculate the predicted change in Δ_{47} at 209 °C after 7 days of heating, and 323 °C after 6 days of heating. We found that only one of the 692 °C fits yielded k_f and $k_{dif\text{-}single}$ values consistent within error of both the temperature in the furnace (±12 °C) and final Δ_{47} datum for the 7 day 209 °C and 6 day 323 °C heats (table 5). Specifically, extrapolation of the rate constants to 209 °C (±12 °C) predicts that heating the optical calcite for 7 days results in no change in Δ_{47} from the starting value, consistent with the experimental observation (table 3). Extrapolation of the rate constants to 323 °C (±12 °C) predicts that heating the optical calcite for 6 days results in a change of Δ_{47} from 0.549 to 0.536 for a 311 °C (−12 °C) heat and 0.506 permil for a 335 °C (+12 °C) heat, which are the ±12 °C range of temperatures for furnace temperature. The modeled Δ_{47} value for the 311 °C heat for 6 days is therefore consistent, within 2σ, with the measured value, 0.560 ± 0.027 permil (2σ). All other fitted parameters predicted changes beyond the 2σ error for this data point. Consequently, we selected this as our 'best' 692 °C fit and used its parameters for all subsequent calculations as given in table 5. However, we note that even this rate constant does predicts a change in Δ_{47} for a 1 week heat at ~320 °C that may slightly over predict the change in Δ_{47} during heating at this temperature range. We ensured that on extrapolation to lower temperatures this issue is not compounded through various example model calculations in later sections (*Modeling and Interpretation of Apparent Equilibrium Blocking Temperatures During Cooling* and *Modeling and Interpretation of Apparent Equilibrium Temperatures During Heating*) and thus that the rate constants are consistent with observations from natural systems.

Clearly, the paired model we present is able to fit our dataset (fig. 8). In particular, the explicit inclusion of pairs of singly substituted species provides a physical mechanism for the kinks observed in many experiments. However, a significant question is whether this model is applicable to other samples and thus can be extended broadly.
To evaluate this, we fit our model to the optical calcite data of Passey and Henkes (2012) and brachiopod data of Henkes and others (2014) (figs. 9 and 10). For the data from Passey and Henkes (2012), we only took the data from their experiments on optical calcites as their spar calcite required a more complex kinetic framework in order for the data to be fit by a kinetic model as discussed previously. Finally, for both studies, we did not fit data from the 385 °C experiments because they appear to only capture the initial, fast kinetics and thus cannot be used to constrain the diffusional rate parameter.

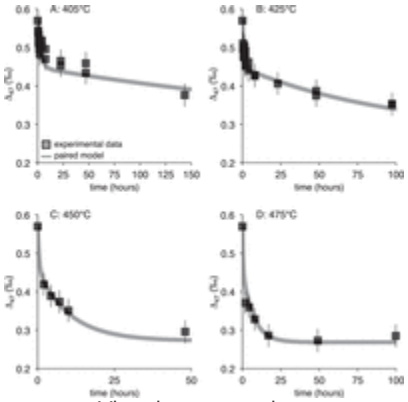

View larger version:

- In this page
- In a new window

Fig. 9.

Paired model as applied to data from optical-calcite heating experiments performed by Passey and Henkes (2012). A) 405 °C data; B) 425 °C data; C) 450 °C data; D) 475 °C data. All Δ_{47} values are presented in the Ghosh reference frame. Error bars are 2 standard errors.

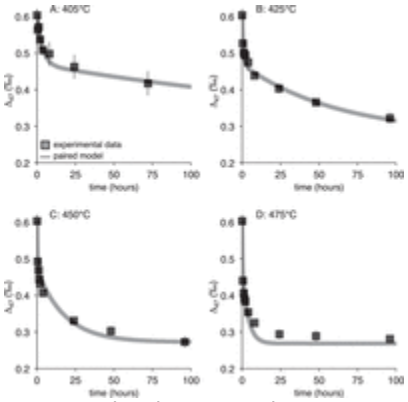

View larger version:

- In this page
- In a new window

Fig. 10.
Paired model as applied to data from brachiopod calcite heating experiments performed by Henkes and others (2014). (A) 405 °C data; (B) 425 °C data; (C) 450 °C data; (D) 475 °C data. All Δ_{47} values are presented in the Ghosh reference frame. These data were converted to the Ghosh reference frame from the absolute reference frame, which is how they were provided in the original study. This was done using the data from Passey and Henkes (2012), which is given in both reference frames, and assuming a linear relationship exists between the two reference frames for a given lab (Dennis and others, 2011). Error bars are 2 standard errors.

Before fitting their experiments, we compared the final, time-invariant values of Passey and Henkes (2012) to those predicted by our high-temperature calibration (fig. 3; table 6). We found that their time-invariant (presumably equilibrated) values are on average 0.011 permil (± 0.002, 1 s.e.) higher than that predicted by our temperature calibration; this is a small multiple of analytical error and likely reflects subtle differences between the Caltech and Johns Hopkins intralab reference frames. As such, we subtracted 0.011 permil from the data of Passey and Henkes (2012) and Henkes and others (2014) before fitting with our paired model. Additionally, one single point was not used in the fits for the Passey and Henkes (2012) 450 °C experimental series (the data point from 24 hours) as it caused modeled rate constants to have errors 30 times greater than the solved-for value.

View this table:

- In this window
- In a new window

Table 6
Comparison of experimental equilibrium Δ_{47} values measured by Passey and Henkes (2012) versus those predicted by our temperature calibration (fig. 3)

Importantly, these fits were made using the same pair excess model as for our measurements using equation (17). Fits are shown in figures 9 and 10 and the derived kinetic parameters are given tables 7 and 8. We compare the kinetic parameters derived from our model from the data of Passey and Henkes (2012)and Henkes and others (2014) to the data presented here in a section below (*Extrapolation of Kinetic Properties to Other Temperatures*) and demonstrate that model yields similar dependencies for the rate constants as a function of temperature.

View this table:

- In this window
- In a new window

Table 7
Rates derived from modeling of optical-calcite heating experiments using data from Passey and Henkes (2012)

View this table:
- In this window
- In a new window

Table 8
Rates derived from modeling of calcitic brachiopod heating experiments using data from Henkes and others (2014)

Extension of the model to apatite.

A critical question is whether our experimental data for the Siilinjarvi apatites heated to various temperatures (fig. 6) shows a kinked time dependence for the changes in Δ_{47} over the course of an experiment. If so, it would advance our hypothesis that non-pseudo-first-order kinetics are a fundamental (or at least common) feature of clumped-isotope-exchange kinetics in carbonate bearing minerals; if not, it would suggest the 'kinked' kinetic behavior is more specific to just calcite. The experiments that produce a time series for heating at 536 °C provide a chance of observing this behavior (that is, because the extent of exchange is neither too small nor too great to obscure the 'kink'), but do not include enough early time points to clearly statistically resolve whether there is a rapid change in Δ_{47} at the start of the experiment. Thus we cannot currently tell if apatites show non-first-order kinetics or not. To understand this will require additional experiments at temperatures between 400 and 500 °C over month-long time scales.

An additional question is how to model the exchange of isotopes of carbonate groups in the apatite lattice. The paired model explicitly describes exchange between a carbonate ion group of interest and the carbonate ion groups surrounding it. For calcites, in which carbonate groups are the major anion, it is straightforward to conceptualize this relationship because each carbonate group generally can only exchange oxygen or carbon by 'trading' with adjoining groups. However, carbonate groups in phosphates are defects and likely surrounded by phosphate groups rather than adjacent carbonate groups. It is unclear to us how to parameterize the geometric elements of our model (that is, the parameter, Z, that describes the number of adjacent exchangeable groups) so that it can be extended to apatite. Here, we simplify the problem by adopting the same parameters as our calcite model; this is likely incorrect but lets us compare the experimental data for apatite and calcite in a self-consistent way. If future experiments demonstrate that apatites have kinetics that differ definitively from the form (that is, time dependence, activation energy) of those for calcites, then an apatite-specific model will need to be constructed.

We only modeled the 536 and 692 °C apatite data (figs. 6B and 6C; table 9) as there is no change in Δ_{47} for the 430 °C experiments beyond the error of the measurements. To fit the 692 °C data for the apatite, which has similar issues as the calcite data at the same temperature, we varied the value used to initialize the fitting routine for the reaction constants and chose the best fit. To check the robustness of our fits, we extrapolated the data as discussed below (in *Extrapolation of Kinetic Properties to Other Temperatures*) to 430 °C and found that the rate constants are in agreement with the experimental data (fig. 6A).

View this table:
- In this window
- In a new window

Table 9

Rates derived from modeling of apatite heating experiments

Our model is able to fit the experimental data from 536 °C and 692 °C. Additionally, and importantly the model parameters, when used to extrapolate the parameters to 430 °C, fit the data within the error of the measurements. Interestingly, these data show slower kinetics at 430 and 536 °C in apatites than in calcites. This is the opposite of what is predicted by the data from carbonatites, in which apatites always have lower apparent equilibrium

temperatures than cogenetic calcites. In other words, the observations from natural samples predicts that apatites should have *faster* kinetics than calcites at a given temperature. Thus the experimental results of the apatites, regardless of the model used, are inconsistent to zeroth order with observations from nature. We address this below (*Modeling and Interpretation of Apparent Equilibrium temperatures During Cooling)* by attributing this difference to the presence of radiation damage in natural apatites that increases diffusion in the lattice, but is annealed away in the experiments, slowing down diffusion and the resultant exchange of isotopes.

MODELS OF APPARENT EQUILIBRIUM TEMPERATURES DURING HEATING AND COOLING

The experiments and models described above can be used to create a general kinetic model for closed-system isotope-exchange reactions in carbonates for any arbitrary time-temperature path. Such a model allows us to ask whether our experimental data and models are consistent with the range of apparent equilibrium temperatures observed in carbonatites and marbles with externally constrained thermal histories, and more generally, their use in studies of thermal histories of carbonate-bearing rocks.

Extrapolation of Kinetic Properties to Other Temperatures

In order to make model calculations at temperatures other than those constrained by experiments, we require a relationship between temperature and rate constant. Generally, rate constants are assumed to be Arrhenian: that is, ln(k) is linearly dependent on 1/T, where T is temperature (Zhang, 2008) and we have adopted that convention here.

The linear fits for ln(k) vs. 1/T are given in figure 11 and include both the fits to data produced in this study as well as for the data given in Passey and Henkes (2012) and Henkes and others (2014) using the paired model derived above. Interestingly, all experiments generated in this study and from Passey and Henkes (2012) and Henkes and others (2014) appear to form a single trend. This is borne out statistically as well: As given in the caption for figure 11, the slopes and intercepts of lines through either all of the data points or only those produced in this study overlap at the 2σ level in all cases. This is significant as it supports the use of a single, unifying model for the kinetics of clumped isotopes in calcites that is independent of starting material.

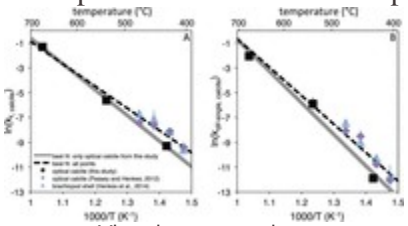

View larger version:

- In this page
- In a new window

Fig. 11.
1/T (Arrhenian) extrapolations of rate constants from calcite data. Errors bars are 2 standard errors. This includes data from experiments performed in this study, by Passey and Henkes (2012), and by Henkes and others (2014). (A) Forward isotope-exchange rate constants (k_f). The slope and intercept of the line fit only to the measurements made in this study (in gray) are −20.7 ± 0.6 (1σ) and 20.1 ± 0.72 (1σ) respectively. The slope and intercept of the best-fit line that passes through all points (the dotted black line) are −17.9 ± 1.2 (1σ) and 17.0 ± 1.7 (1σ) respectively. Thus the intercepts and slopes all overlap at the 2σ level (though for the slopes only the error bars overlap). (B) Diffusion rate constants for singletons ($k_{dif\text{-}single}$). The slope and intercept of the line fit only to the measurements made in this study (in gray) are −25.4 ± 3.7 (1σ) and 24.7 ± 4.5 (1σ) respectively. The slope and intercept of the best-fit line that passes through all points (the dotted black line) are −22.9 ± 1.9 (1σ) and 22.3.0 ± 2.5. As was the case in (A), the intercepts and slopes all overlap at the 2σ level.

Consequently, we suggest that the paired model presented here accurately describes the atomistic basis for the seemingly complex behavior of experimental clumped-isotope re-equilibration and can be extrapolated beyond our specific sample. However, the spar calcite of Passey and Henkes (2012)clearly has distinct kinetics from the three samples modeled here, which requires that there will be different required kinetics for some samples. One possible explanation for this, as given by Passey and Henkes (2012), is that the trace element content of a sample can control the observed reaction rates. Alternatively, if the spar calcite of Passey and Henkes (2012) has a different starting abundance of pairs (specifically less) than would be predicted by this model, it would exhibit the more rapid kinetics observed for the sample.

Although all of the fits to the different data sets presented in figure 11 are statistically identical, inclusion of the Passey and Henkes (2012) and Henkes and others (2014) data causes the slopes (that is, the activation energies) of the fits to be slightly shallower than suggested by our data alone. Use of these shallower lines predicts significant changes in Δ_{47} values at 323 °C (±12) over laboratory time scales (6 days) that are beyond the error of our experiments. In order to be as consistent with our data set as possible, we perform all calculations in the subsequent sections using the line defined by our data. This difference demonstrates the inherent challenge of extrapolating kinetic results generated at elevated temperatures to geologically relevant conditions — even subtle differences between experimental measurements may be magnified to large predicted differences at geological conditions.

The Arrhenian relationships defined for our optical calcite with 1σ errors are:

$$\ln(k_{f,\,calcite}) = \frac{-20700\,(\pm 600)}{T} + 20.1\,(\pm 0.7),\ (r^2 = 1.00) \quad (18)$$

$$\ln(k_{dif\text{-}single,\,calcite}) = \frac{-25400\,(\pm 3700)}{T} + 24.7\,(\pm 4.5),\ (r^2 = 0.98) \quad (19)$$

All rate constants have units of sec^{-1}. The temperature at which $k_{f,\,calcite}$ and $k_{dif\text{-}single,\,calcite}$ are equal is 740 °C. At lower temperatures, $k_{dif\text{-}single,\,calcite}$ is less than $k_{f,\,calcite}$. This indicates that, for all geologically relevant temperatures, diffusional splitting and forming of pairs is the overall rate-limiting step for the generation and destruction of $^{13}C^{16}O_2{}^{18}O^{2-}$ groups. The slopes of these lines yield activation energies of 172 (±5, 1σ) and 211 (±30, 1σ) kJ/mole for exchange and diffusion in calcites respectively. Activation energies of self-diffusion of oxygen in calcites have been measured for dry experiments to be between 242 to 261 kJ/mol by Labotka and others (2000 and 2004) depending on the pressure and ~380 kJ/mol by Anderson (1969) as given in Labotka and others (2000) or 412 kJ/mol as given in Farver (2010). In hydrous experiments this diffusivity was found to be 173 kJ/mole by Farver (1994). Activation energies for the diffusion of carbon in dry experiments are measured to vary from 166 kJ/mol to 291 kJ/mol by Labotka and others (2000 and 2004) with a dependence on the pressure used in the experiment, and 71 kJ/mol for 250 to 550 °C experiments on unannealed calcites and 368 kJ/mol for experiments above 550 °C on both pre-annealed and unannealed calcites by Anderson (1969). In hydrous experiments, carbon diffusion was found to be 364 kJ/mol by Kronenberg and others (1984). Thus our measurement is in the range of reported self-diffusivities of carbon and oxygen in calcites and within 2σ error for similarly 'dry' experiments.

As discussed in Passey and Henkes (2012), it is not straightforward to make a direct comparison of the kinetics of isotope exchange reactions that determine the rates of change of Δ_{47} values to the results of experiments designed to calculate the diffusivity of O and C. Specifically, the direct comparison of the activation energies derived here to those for the experimental determination of diffusivities using tracers introduced at the surface of the mineral (as was done in all of the studies discussed) may be misleading. This is because diffusion through a surface may be controlled by reactions at the interface between the tracer and the calcite (Labotka and others, 2004; Labotka and others, 2011) that could be unrelated to the results determined in our experiments which are dominantly controlled by reactions and diffusion within the crystal (Passey and Henkes, 2012). This is discussed further in the section *Model Caveats and a Comparison to Diffusion Experiments* below.

We performed similar extrapolations for the phosphate dataset using the 530 and 692°C experiments. The equations are:

$$\ln(k_{f,\ apatite}) = \frac{-23700}{T} + 21.5 \quad (20) \ln(k_{dif\text{-}single,\ apatite}) = \frac{-26100}{T} + 23.8 \quad (21)$$

No correlation coefficient or errors are given as they are all two point fits. The temperature at which $k_{f,\ apatite}$ and $k_{dif\text{-}single,\ apatite}$ is equal to 740 °C. At lower temperatures, $k_{dif\text{-}single,\ apatite}$ is less than $k_{f,\ apatite}$. Why k_f,and $k_{dif\text{-}single}$ would be equal at the same temperature for both calcite and apatite is not clear but may reflect, in part the challenge of fitting the 700 °C data, which, for both samples, converges to the equilibrium value within minutes. The activation energies are 197 and 217 kJ/mole for exchange and diffusion. To our knowledge, the only study on oxygen diffusion in apatites, which was hydrous, yielded an activation energy of 125 or 205 kJ/mole depending on the crystallographic axis examined (Farver and Giletti, 1989).

Modeling and Interpretation of Apparent Equilibrium Blocking Temperatures During Cooling

We used equations (18) and (19) to model the apparent equilibrium blocking temperature recorded by calcite for a variety of modeled cooling histories. Because previous studies have established common values for apparent equilibrium blocking temperatures for slowly uplifted metamorphic rocks and carbonatites (~125 to 280 °C; Ghosh and others, 2006; Dennis and Schrag, 2010; Bonifacie and others, 2011; Bonifacie and others, 2013), we have some basis for deciding whether the predictions of these models are reasonable. In other words, natural samples with relatively simple, constrained cooling histories can test the plausibility of the extrapolation of the model and kinetic parameters to geologically relevant thermal histories. For these models, we began with a bulk stable-isotope composition identical to the optical calcite used. We then subjected the sample to a modeled temperature history that first includes initial heating to 350 °C for 10,000 years to ensure pairs and singletons were fully equilibrated at high temperatures. After this, we calculated the consequences of cooling the samples down to 0 °C at linear rates ranging from 10,000 °C to 1 °C per million years (fig. 12A).

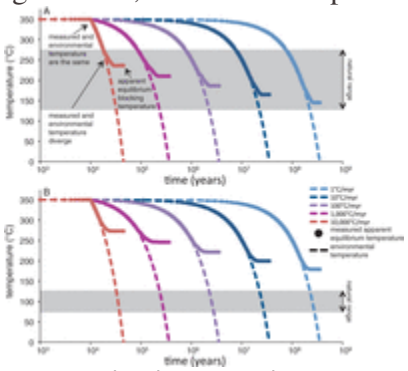

View larger version:

- In this page
- In a new window

Fig. 12.

Apparent equilibrium temperatures derived from modeled parameters. Dashed lines are the environmental temperature while solid points are the recorded apparent equilibrium temperatures. The gray zone indicates the area where samples that have cooled over geologically time generally are found. (A) Calcites; (B) Apatites.

Our model predicts rapidly cooled samples (10,000-1000 °C/myr) will have apparent equilibrium temperatures from 235 to 210 °C and more slowly cooled samples (100 to 1 °C/myr) from 185 to 145 °C. Our results for calcites from carbonatites (~190 °C to 125 °C) resemble the range predicted from the model. In particular, the Oka body was independently estimated to have cooled around 1000 °C per million years based on oxygen-isotope thermometry of multiple minerals (Haynes and others, 2002). Its apparent equilibrium blocking temperature for carbonate minerals is 192 ± 4°C (1σ) and is similar to the predicted apparent equilibrium temperature of 210 °C for the 1000°C/myr cooling rate. However, some carbonatites record temperatures of ~250 °C and can goes as high as 293 °C (Dennis and Schrag, 2010). These results suggest either exceptionally rapid cooling rates for these materials, that under some circumstances the reaction rates that control reordering of carbonate apparent equilibrium

temperatures may be slower than we found in our experiments, or that these samples represent some disequilibrium phenomenon. Additionally, the mineralogy of the carbonatites could be of importance as dolomites and calcites appear to have distinct kinetics (Bonifacie and others, 2011; Eiler, 2011; Ferry and others, 2011).

Additionally, we routinely measure a Carrara marble as an internal standard; this material has a long term average apparent equilibrium temperature of 206 °C. The Carrara marble is predicted to have cooled between 10 to 16 °C per million years (myr) from 11 Ma to 6 Ma and 38 to 55 °C/myr from 6 to 4 Ma using fission track and U/Th-He thermochronology and fission track apatite thermochronology (Balestrieri and others, 2003 and references therein). Based on these cooling histories, Passey and Henkes (2012) estimated that cooling from 10 to 16 °C/myr occurred at temperatures between 200 and 250 °C while cooling from 38 to 55 °C/myr occurred at temperatures from 200 to 120 °C. Our models predict apparent equilibrium temperatures for 10 and 100 °C per million years as 165 °C and 185 °C degrees respectively, which, although similar to the measured apparent blocking temperatures, are lower than would be predicted using the cooling rates derived from thermochronology studies. Calcite in marbles generally preserve apparent equilibrium temperatures from 150 to 200 °C (Bonifacie and others, 2011; Eiler, 2011) and have cooling rates between 1 to 100 °C/myr. Consequently, the model is broadly consistent with data from marbles. We note that the Oka carbonatite is thought to have cooled at least an order of magnitude faster than the Carrara marble sample, but the Oka sample has a lower measured apparent equilibrium temperature than the Carrara marble. Thus, no simple model will ever be able to reconcile the apparent equilibrium temperatures of both of these particular samples with the given independently estimated cooling histories.

Nevertheless, our model predictions of reaction rates bound the range of apparent temperatures observed in most natural marbles and carbonatites with reasonable modeled geological cooling rates (fig. 12A). We consider it likely that some of the disagreements between the model and observations stem from our simple assumptions (that is, linear cooling rates; simple, single-phase cooling histories; no recrystallization during cooling). Greater complexity must be present in some of the studied samples. For this reason, we are generally encouraged by this comparison, as it suggests that rates observed in the laboratory are at least generally consistent with observations of natural samples. An additional test of our model and kinetic parameters could be accomplished through the measurement of a suite of related samples with well-constrained and simple thermal histories, such as carbonates near small igneous intrusions. Comparison of model predictions using equations (20) and (21) with natural samples in the case of apatite yields a different result. Figure 12B presents the predicted apparent equilibrium temperatures of carbonate clumped-isotope compositions of apatites for various cooling rates. In all cases we considered, apatites are predicted to have higher apparent equilibrium temperatures as compared to identically cooled calcites. This is in complete disagreement with natural samples. We suggest two possible explanations for this behavior:

1. The model may not capture the kinetics of how carbonate groups exchange isotopes in apatites. Our model for carbonate exchange and diffusion in apatites could be missing key physical parameters such as the local exchange of oxygen between PO_4^{3-} and CO_3^{2-} groups. This would require an entirely different model that describes the kinetics of exchange and diffusion of isolated carbonate groups within an apatite lattice.
2. All apatite samples that were heated as part of this study likely contain radiation damage generated from alpha emission and heavy-daughter product recoil during decay of radioactive elements like U and Th and spontaneous fission of U. The presence of damage in a crystal lattice is known to affect the diffusivities of various elements: for example He diffusion in apatite is lowered in radiation damaged apatites (Farley, 2000; Shuster and others, 2006), but enhanced for Pb in zircons (Cherniak and others, 1991).

Based on fission-track studies in apatites, this damage is fully annealed away within 20 minutes at 400 °C (Green and others, 1986). We hypothesize that these defects enhance reaction/diffusion rates in radiation-damaged natural apatites, and their removal by annealing in our experiments decreases these rates, yielding slower kinetics of reordering than actually occurs in natural, radiation-damaged apatite. Effectively, we suggest the hypothesis of Passey and Henkes (2012), while not part of our model for clumped-isotope reordering of calcite, plays an

important role in reordering in apatite in which observable structural damage is created in samples and routinely documented.

Some support for this second hypothesis can be found in the experiments of Cherniak and others (1991), who studied diffusivities of lead using a surface tracer implantation technique, which generates extensive lattice damage. They found that their observed diffusivities in apatite at temperatures above 600 °C were similar to previous results generated by a method that does not create artificial lattice damage, whereas their measured diffusivities in zircon were faster than previously observed using these alternate methods. They hypothesized that because apatites anneal structural damage rapidly at the experimental temperatures (600 °C), the damaged induced by introduction of Pb into the surface had no effect on the measured diffusivities. Zircon, on the other hand could not anneal the damage resulting in rapid diffusion of lead in the surface compared to experiments that introduced lead without damaging the lattice.

By analogy to the experiments of Cherniak and others (1991), we propose that natural apatites possess radiation damage that increases their rate of reordering of clumped-isotope compositions at low temperatures (<250 °C) near the nominally measured apparent equilibrium temperatures in apatite and calcite. In our experiments at higher temperature (>400 °C) this damage was quickly annealed away reducing the diffusivity of carbonate groups or oxygen in the apatite lattice. If correct, this suggests that the apparent equilibrium temperature of the carbonate clumped-isotope thermometer in apatite could be sensitive not only to the thermal history of the sample, but also to its uranium and thorium content and age. More studies on apatites will be needed to explore this hypothesis. For example, igneous apatites with high and low amounts of uranium and thorium and known thermal histories could be compared to see if increased potential for damage changes the apparent equilibrium temperature.

Modeling and Interpretation of Apparent Equilibrium Temperatures During Heating

We also modeled the changes in calcite apparent equilibrium temperatures that should accompany the heating of a sample that formed in internal isotopic equilibrium near Earth surface temperatures for geologically relevant timescales. We did this by initializing calcites with an apparent equilibrium temperature of 25 °C, initial overabundance of pairs derived from equation (17), and bulk isotopic compositions equal to the average values for our optical calcite starting material. We then calculated the consequences of heating each sample instantaneously to a constant temperature for one hundred million years. Results of these calculations for calcite are presented in figure 13. Our model predicts that measurable changes in the apparent equilibrium temperature do not occur below 75 °C. Full equilibration is not reached until the sample is heated above ~175 °C in this time frame.

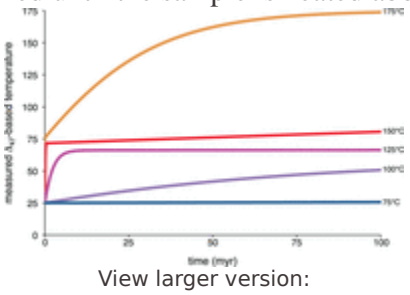

View larger version:

- In this page
- In a new window

Fig. 13.

Change in apparent equilibrium temperatures for calcites with originally low (25 °C) apparent equilibrium temperatures due to heating. Temperatures given to the right next to each line are the temperatures the sample was exposed to in the model. ‘myr’ signifies millions of years.

Of interest is that the predicted temperature changes occur in two distinct steps: increases in environmental temperatures to below 125 °C after 100 million years partially alter the clumped temperature recorded within a few

tens of millions of years but then cease changing, reaching a steady-state value below the actual ambient temperature. If the temperature is increased above 125 °C, an initial rapid increase in apparent equilibrium temperature occurs, followed by a slower increase until the ambient, environmental temperature is reached (fig. 13). This two-stage change in apparent equilibrium temperature is the result of the explicit inclusion of pairs as a distinct population of isotopic species in the model, which act to buffer the creation and destruction of clumped species as discussed above in the *Model Intuition* section.

Theses models predict something potentially important regarding the nature of the clumped-isotope record of ancient carbonates: we suggest that the relatively rapid kinetics of reaction between 'clumps' and 'pairs', combined with the relatively slow diffusive splitting of pairs at low temperatures, means that sedimentary carbonates exposed to moderate burial temperatures (~80–100 °C) can undergo small increases in measured apparent equilibrium temperatures (of order 0–25 °C), which are then stabilized for long periods of time. It is not until higher burial temperatures (above ~150 °C) that apparent equilibrium temperatures begin to approach the ambient temperature over geological timescales. This effect, if it really occurs in natural carbonates, could be a key systematic error in the interpretation of carbonate clumped-isotope data for ancient, deeply buried platform limestone sequences. This is a particularly important consideration for systems with maximum burial temperatures in the range ~60 to 100 °C where conventional signs of burial metamorphism are subtle but temperatures are high enough to permit partial resetting. This effect is particularly insidious because the temperature will not continuously increase monotonically with time as is generally expected, but can instead stabilize at a higher temperature than formation, but lower temperature than the burial temperature. These effects may be difficult to diagnosis unless detailed thermal histories of the rocks are known.

A potential way to understand these effects is to make measurements on phosphates and calcites from the same bed of rocks precipitated in similar conditions (for example, calcitic vs. phosphatic brachiopods). Although the kinetics of exchange in phosphates are clearly complex, it appears they behave differently from calcites in natural rocks. As such, one could measure both and, if they give the same temperature, have increased confidence that that temperature represents a primary signal. Similar principles may apply to other mineral pairs (for example, calcite with aragonite or dolomite).

Although experiments from this study, Passey and Henkes (2012), and Henkes and others (2014) demonstrate that on heating, apparent equilibrium temperatures initially increase rapidly followed by a slower increase, a critical question is whether the initial rapid 'jump' in measured temperature occurs in samples from natural systems heated at geologically relevant rates. For example, Henkes and others (2014) concluded that the early, faster kinetics that form the initial portion of the kinks observed in experimental data are not particularly important for the interpretation of samples, with burial histories below ~150 °C, while our model predicts that it is between the range of 75 to 150 °C that the rapid portion of the kinetics are manifested and important. To explore this, we compared our model to a clumped-isotope study of paleosols from the Siwalik Group in Nepal that experienced a simple, well constrained thermal history (Quade and others, 2013). In this study, all samples are from paleosols that formed within a few meters of the Earth's surface (and thus have a limited range of initial temperatures), were buried between 0 and 5 km within ~10 to 12 million years and then rapidly uplifted to the surface. An observation of the data from Quade and others (2013), is that samples that never experienced burial temperatures above ~200 °C and did not, based on petrographic arguments, recrystallize, give temperatures too hot by ~10 to 30 °C to be interpreted as surface formation temperatures. Additionally, samples buried more deeply (>~2km) appear to give higher temperatures than more shallowly (<~2km) buried samples (fig. 14).

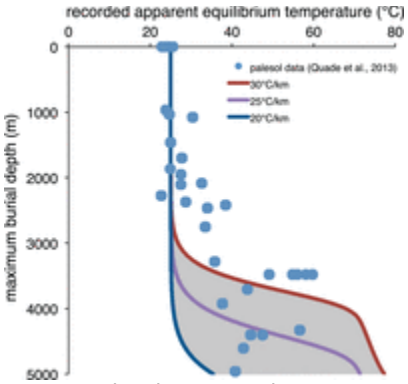

View larger version:

- In this page
- In a new window

Fig. 14.
Paired model applied to paleosol data from the Siwalik Basin, Nepal (Quade and others, 2013). Samples are assumed to have been buried to depths between 0 and 5 km at a rate of 0.5 km/million years. These burial histories are converted to thermal histories by assuming a 20, 25, or 30 °C/km geotherm. The gray area represents the predicted range of temperatures given the geothermal gradients in the vicinity.

To explore whether these 'high' temperatures could be explained by our model, we modeled a simple burial history in which the paleosols samples form at the surface of the Earth at 25 °C (the average apparent equilibrium temperature of modern paleosols from the study area), with a concentration of pairs calculated from equation (17). Samples were then assumed to have been buried between 0 and 5 km (the maximum burial depth) with a linear burial rate with time where the oldest, deepest samples are assumed to be 10 million years old. Samples were finally returned to the surface (still at 25 °C) instantaneously. We converted these burial histories into thermal histories by assuming geotherms of 20, 25, and 30 °C/km, which are the published range of geotherms for the Siwalik Basin (Khan and Raza, 1986) and modeled the expected change in temperature of the samples vs. maximum burial depth (fig. 14).

The modeled apparent equilibrium temperatures match the form of the observed apparent equilibrium temperatures. Specifically, we predict no change in temperature for the first 3 km, consistent with the data, followed by a shift in measured temperature between 3 to 4.5 km (burial temperatures of ~100 °C). For the 25 and 30 °C/km geotherms, the measured temperatures stabilize or increase at a markedly slower rate with further burial between 4 to 5 km depth. Although a single geotherm does not fit all the data, such a fit is impossible for this data set given the spread in measured temperatures. This spread is presumably related not only to post-depositional transformations as modeled here, but also do the large variation in temperatures of paleosol deposition (>10 °C variability in a single site) due to differences of shading, timing of precipitation, and depth of precipitation (Passey and others, 2010; Peters and others, 2013; Quade and others, 2013). Critically, the model appears to be consistent with a real system with a known and simple burial history demonstrating that it can be used to model thermal histories and generate reasonable results. Furthermore, this test is consistent with rapid 'jumps' in apparent equilibrium temperatures of ~10 to 30 °C during burial from ~80 to 100 °C being a real phenomenon.

Model Caveats and a Comparison to Diffusion Experiments

All the models presented above should be approached with some caution because their predictions are based on extrapolation of experimental data to low temperatures, and depend on the consequences of a hypothesized population of 'pairs' that are diffusionally split into singeltons in carbonates. Specifically, it is important to realize that changing our proposed model of pairs [that is, their temperature dependent abundance described by equation (17)] would significantly alter the predicted kinetics of isotopic reordering, in some cases even allowing for 'overshoots' of apparent equilibrium temperature on heating where rapid heating causes measured apparent

equilibrium temperatures recorded to be temporarily higher than the physical temperature. Certain initial overabundances of pairs can also cause heating to actually lower the recorded temperature (as the extra pairs back react more than the clumped species split). It is unclear if such kinetics occur in natural samples.

Despite these caveats, we reemphasize that the models describe the complex kinetics of our experiments and those of Passey and Henkes (2012) and Henkes and others (2014), predict apparent equilibrium temperatures during cooling that bracket the range of measured temperatures in natural igneous and metamorphic calcites, and provide a reasonable fit to real samples that have undergone burial and exhumation. Thus, we believe the model behaviors we demonstrate are a useful guide to understanding how changes in physical temperature affects recorded apparent equilibrium temperatures in calcites and apatites. A key insight to be taken away from the model is that heating of samples does not lead to simple kinetics. Rather small (order 10 °C), but rapid increases in the temperature recorded by samples initially precipitated or recrystallized at near-surface temperatures may occur.

The model does not include certain physical parameters that are thought to influence the kinetics of diffusion of oxygen and carbon in calcites and apatites. For example, defects, trace element content, water fugacity, and pressure are all hypothesized or documented to influence diffusion (Anderson, 1969; Kronenberg and others, 1984; Farver and Giletti, 1989; Farver, 1994; Labotka and others, 2000; Labotka and others, 2004; Labotka and others, 2011). At an even more basic level, it is important to consider what species or atoms are actually diffusing in calcites and apatites. The paired model presented here involves distinct carbonate groups in the lattice interacting and diffusing. This is an acceptable model for dry, low-pressure experiments such as those used in Passey and Henkes (2012) and Henkes and others (2014) in which C and O are hypothesized to diffuse together in carbonate groups (Anderson, 1969; Labotka and others, 2000; Labotka and others, 2004).

However, oxygen and carbon self-diffusion in calcite have a complex dependence on water fugacity (Kronenberg and others, 1984; Farver, 1994; Labotka and others, 2011), presence of defects (Anderson, 1969; Kronenberg and others, 1984; Farver, 1994), pressure (Labotka and others, 2000; Labotka and others, 2004), and possibly trace metal content (Kronenberg and others, 1984; Farver, 1994) and they can be decoupled in these circumstances from each other. Specifically, oxygen self-diffusion is typically enhanced relative to carbon in the presence of high pressures or elevated water fugacities requiring that oxygen diffuses as a different species (for example, as O) than carbon (Anderson, 1969; Kronenberg and others, 1984; Farver and Giletti, 1989; Farver, 1994; Labotka and others, 2000; Labotka and others, 2004; Labotka and others, 2011). However, Passey and Henkes (2012) showed that clumped-isotope exchange rates at 100 MPa are identical, within error, to 0.1 MPa experiments. Furthermore, the 100 MPa experiments of Passey and Henkes (2012) were conducted in the presence of water and had identical reaction rates as low pressure (0.1 MPa), dry experiments. Consequently, as discussed by Passey and Henkes (2012), it may not be straightforward to incorporate insights from diffusion experiments of O and C into clumped-isotope-exchange kinetics.

SUMMARY AND CONCLUSIONS

We made measurements and conducted experiments aimed at understanding the kinetics of clumped-isotope reordering in calcites and apatites as a function of time and temperature. Measurements of carbonatite samples demonstrate that apatites consistently yield lower apparent equilibrium temperatures than co-occurring carbonate minerals. In the carbonatites, it is observed that the apparent equilibrium temperatures for both calcite and apatite correlate to the emplacement depth of the intrusion. Apparent equilibrium temperatures range from 60 to 130 °C in apatites and 125 to 190 °C for carbonate minerals (dominantly made of calcite). The results for the carbonate minerals are consistent with previous studies of apparent equilibrium temperatures of carbonatites and marbles (Ghosh and others, 2006; Dennis and Schrag, 2010; Bonifacie and others, 2013). This suggests that apatites from natural settings have lower apparent equilibrium blocking temperatures than carbonate minerals.

To better understand the results from natural systems, we performed heating experiments on calcite and apatite minerals between 200 and 700 °C. As seen by others (Passey and Henkes, 2012; Henkes and others, 2014), these experiments demonstrate that calcites exhibit complex (that is, non-pseudo-first-order) kinetics. Additionally, in experiments apatites change in clumped-isotope compositions more slowly than calcites, opposite what was observed in nature. Whether apatites also display complex kinetics is unclear and will have to be explored through more experiments. To explain the results of our experiments, we developed a model that incorporates both reaction and diffusion in mineral lattices. This model allows for complex kinetics and describes the features present in our data and similar results from previous related work. Extrapolation of the data is consistent with natural, slowly cooled carbonate minerals both from carbonatites (Dennis and Schrag, 2010) and marbles (Ghosh and others, 2006; Bonifacie and others, 2011). Observations from naturally occurring apatites and from experiments are in disagreement, which may be related to annealing of radiation damage when natural apatites are exposed to high temperatures in our experiments.

Our model predicts a potentially important feature of heating on measured Δ_{47}-based temperatures. Specifically, the heating of rocks will not necessarily increase the apparent equilibrium temperature monotonically. Rather, at lower temperatures (~80 to 100 °C), a small change of order 10 °C in recorded temperature occurs and then is stabilized. Not until higher temperatures (~>150 °C) does a sample change its recorded temperature significantly throughout its burial history. This model is in agreement with the observed changes in apparent equilibrium temperature of paleosols from the Siwalik Group, Nepal which experienced a simple thermal history with burial temperatures up to ~150 °C. This work has implications for our interpretation of samples that give warm temperatures for past environments, as well as for understanding cooling and heating paths for metamorphic systems. Specifically, if correct, it suggests that ancient samples formed at low temperatures (for example, 25 °C) that experienced moderate thermal histories (for example, ~80–100 °C) can change in apparent equilibrium temperatures by ~25 °C, and then stabilize at that change. Thus the presence of moderately but not exceptionally high apparent equilibrium temperatures (30–50 °C) in ancient fossils may be the result of internal isotope-exchange reactions that will have no effect on the lattice or trace-element content of the minerals, which are commonly used to diagnosis the presence diagenesis.

ACKNOWLEDGMENTS

We thank George Rossman for providing us with the optical calcite and Keith Bell for providing us with carbonates from Kovdor. We thank Chi Ma for assistance with electron microprobe measurements. This paper benefitted from discussions with Itay Halevy. We thank Youxue Zhang, David Shuster, and Matt Kohn for incredibly helpful, detailed reviews. We additionally thank our Associate Editor John Valley and Editor Page Chamberlain for helpful suggestions and editorial handling. DAS was supported by an Eaton Fellowship from Caltech and a Graduate Research Fellowship from the National Science Foundation. JME was funded by the National Science Foundation.

Footnotes

- ↵1 $^{i}\delta=1000*(^{i}R_{sample}/^{i}R_{std}-1)$; $^{13}R=[^{13}C]/[^{12}C]$ $^{18}R=[^{18}O]/[^{16}O]$; the standard (std) is VPDB for carbon-isotope measurements and VSMOW for oxygen-isotope measurements.
- ↵2 $^{47}\delta=1000*(^{47}R_{sample}/^{47}R_{std}-1)$; $^{47}R=[^{47}CO_2]/[^{44}CO_2]$; the standard (std) is our working gas.
- ↵3 The probability of a $^{12}C^{16}O_2{}^{18}O^{2-}$ group neighboring a $^{13}C^{16}O_3{}^{2-}$group in a calcite lattice is calculated as follows: We assume that a given carbonate group is surrounded by 6 other groups in the calcite lattice (see text). Therefore the probability that a $^{12}C^{16}O_2{}^{18}O^{2-}$ is *not* next to at least one $^{13}C^{16}O_3{}^{2-}$ group is $(1-0.01)^6 = 0.94$. Here 0.01 is the probability of any given carbonate group being $^{13}C^{16}O_3{}^{2-}$. Thus the probability that a $^{12}C^{16}O_2{}^{18}O^{2-}$ group neighbors at least one $^{13}C^{16}O_3{}^{2-}$ is 1–0.94 = 0.06, or 6%.

Previous Section

REFERENCES

Affek H. P.
, 2013, Clumped isotopic equilibrium and the rate of isotope exchange between CO_2 and water: American Journal of Science, v. **313**, n. 4, p. 309–325,doi:http://dx.doi.org/10.2475/04.2013.02

Anderson T. F.
, 1969, Self-diffusion of carbon and oxygen in calcite by isotope exchange with carbon dioxide: Journal of Geophysical Research, v. **74**, n. 15, p.3918–3932, doi:http://dx.doi.org/10.1029/JB074i015p03918

Balestrieri M. L.,
Bernet M.,
Brandon M. T.,
Picotti V.,
Reiners P.,
Zattin M.
, 2003,Pliocene and Pleistocene exhumation and uplift of two key areas of the Northern Apennines: Quaternary International, v. **101–102**, p. 67–73,doi:http://dx.doi.org/10.1016/S1040-6182(02)00089-7

Banner J. L.,
Hanson G. N.
, 1990, Calculation of simultaneous isotopic and trace element variations during water-rock interaction with applications to carbonate diagenesis: Geochimica et Cosmochimica Acta, v. **54**, n. 11, p. 3123–3137,doi:http://dx.doi.org/10.1016/0016-7037(90)90128-8

Blank J. G.,
Stolper E. M.,
Carroll M. R.
, 1993, Solubilities of carbon dioxide and water in rhyolitic melt at 850 °C and 750 bars: Earth and Planetary Science Letters, v.**119**, n. 1–2, p. 27–36, doi:http://dx.doi.org/10.1016/0012-821X(93)90004-S

Bonifacie M.,
Ferry J. M.,
Horita J.,
Vasconcelos C.,
Passey B. H.,
Eiler J. M.
, 2011,Calibration and applications of the dolomite clumped isotope thermometer to high temperatures: Mineralogical Magazine, v. **75**, n. 3, p. 551.

Bonifacie M.,
Calmels D.,
Eiler J.
, 2013, Clumped isotope thermometry of marbles as an indicator of the closure temperatures of calcite and dolomite with respect to solid-state reordering of C–O bonds: Mineralogical Magazine, v. **77**, n. 5, p. 735.

Came R. E.,
Eiler J. M.,
Veizer J.,
Azmy K.,
Brand U.,
Weidman C. R.
, 2007,Coupling of surface temperatures and atmospheric CO_2 concentrations during the Palaeozoic era: Nature, v. **449**, p. 198–201, doi:http://dx.doi.org/10.1038/nature06085

Cherniak D. J.,
Lanford W. A.,
Ryerson F. J.
, 1991, Lead diffusion in apatite and zircon using ion implantation and Rutherford backscattering techniques: Geochimica et Cosmochimica Acta, v. **55**, n. 6, p. 1663–1673, doi:http://dx.doi.org/10.1016/0016-7037(91)90137-T

Cherniak D. J.,
Hervig R.,
Koepke J.,
Zhang Y.,
Zhao D.
, 2010, Analytical methods in diffusion studies, *in* Zhang Y., Cherniak D. J., editors, Diffusion in Minerals and Melts: Reviews in Mineralogy and Geochemistry, v. **72**, p. 107–170,doi:http://dx.doi.org/10.2138/rmg.2010.72.4

Clog M.,
Stolper D.,
Eiler J. M.

, 2015, Kinetics of $CO_{2(g)}$–$H_2O_{(l)}$ isotopic exchange, including mass 47 isotopologues: Chemical Geology, v. **395**, p. 1–10,doi:http://dx.doi.org/10.1016/j.chemgeo.2014.11.023
Criss R. E.
, 1999, Principles of Stable Isotope Distribution: New York, Oxford University Press, 264 p.
Cummins R. C.,
Finnegan S.,
Fike D. A.,
Eiler J. M.,
Fischer W. W.
, 2014,Carbonate clumped isotope constraints on Silurian ocean temperature and seawater $\delta^{18}O$: Geochimica et Cosmochimica Acta, v. **140**, p. 241–258,doi:http://dx.doi.org/10.1016/j.gca.2014.05.024
Denbigh K. G.
, 1981, The principles of chemical equilibrium: with applications in chemistry and chemical engineering: New York, Cambridge University Press, 4th Edition, 520 p.
Dennis K. J.,
Schrag D. P.
, 2010, Clumped isotope thermometry of carbonatites as an indicator of diagenetic alteration: Geochimica et Cosmochimica Acta, v. **74**, n. 14, p. 4110–4122, doi:http://dx.doi.org/10.1016/j.gca.2010.04.005
Dennis K. J.,
Cochran J. K.,
Landman N. L.,
Schrag D. P.
, 2013, The climate of the Late Cretaceous: New insights from the application of the carbonate clumped isotope thermometer to Western Interior Seaway macrofossil: Earth and Planetary Science Letters, v. **362**, p. 51–65, doi:http://dx.doi.org/10.1016/j.epsl.2012.11.036
Dennis K. J.,
Affek H. P.,
Passey B. H.,
Schrag D. P.,
Eiler J. M.
, 2011, Defining an absolute reference frame for ‘clumped’ isotope studies of CO_2: Geochimica et Cosmochimica Acta, v. **75**, n. 22, p. 7117–7131,doi:http://dx.doi.org/10.1016/j.gca.2011.09.025
Dodson M. H.
, 1973, Closure temperature in cooling geochronological and petrological systems: Contributions to Mineralogy and Petrology, v. **40**, n. 3, p. 259–274, doi:http://dx.doi.org/10.1007/BF00373790
Douglas P. M. J.,
Affek H. P.,
Ivany L. C.,
Houben A. J. P.,
Sijp W. P.,
Sluijs A.,
Schouten S.,
Pagani M.
, 2014, Pronounced zonal heterogeneity in Eocene southern high-latitude sea surface temperatures: Proceedings of the National Academy of Sciences of the United States of America, v. **111**, n. 18, p. 6582–6587,doi:http://dx.doi.org/10.1073/pnas.1321441111
Eagle R. A.,
Schauble E. A.,
Tripati A. K.,
Tütken T.,
Hulbert R. C.,
Eiler J. M.
, 2010,Body temperatures of modern and extinct vertebrates from ^{13}C-^{18}O bond abundances in bioapatite: Proceedings of the National Academy of Sciences of the United States of America, v. **107**, n. 23, p. 10377–10382,doi:http://dx.doi.org/10.1073/pnas.0911115107
Eagle R. A.,
Tütken T.,
Martin T. S.,
Tripati A. K.,
Fricke H. C.,
Connely M.,
Cifelli R. L.,
Eiler J. M.
, 2011, Dinosaur body temperatures determined from isotopic (^{13}C-^{18}O) ordering in fossil biominerals: Science, v. **333**, n. 6041, p. 443–445,doi:http://dx.doi.org/10.1126/science.1206196

Eiler J. M.
, 2007, “Clumped-isotope” geochemistry - The study of naturally-occurring, multiply-substituted isotopologues: Earth and Planetary Science Letters, v.**262**, n. 3–4, p. 309–327, doi:http://dx.doi.org/10.1016/j.epsl.2007.08.020
Eiler J. M.
, 2011, Paleoclimate reconstruction using carbonate clumped isotope thermometry: Quaternary Science Reviews, v. **30**, n. 25–26, p. 3575–3588,doi:http://dx.doi.org/10.1016/j.quascirev.2011.09.001
Epstein S.,
Buchsbaum R.,
Lowenstam H. A.,
Urey H. C.
, 1953, Revised carbonate-water isotopic temperature scale: Geological Society of America Bulletin, v. **64**, n. 11, p. 1315–1326, doi:http://dx.doi.org/10.1130/0016-7606(1953)64[1315:RCITS]2.0.CO;2
Farley K. A.
, 2000, Helium diffusion from apatite: General behavior as illustrated by Durango fluorapatite: Journal of Geophysical Research: Solid Earth (1978–2012), v.**105**, n. B2, p. 2903–2914.
Farver J. R.
, 1994, Oxygen self-diffusion in calcite: Dependence on temperature and water fugacity: Earth and Planetary Science Letters, v. **121**, n. 3–4, p. 575–587,doi:http://dx.doi.org/10.1016/0012-821X(94)90092-2
Farver J. R.
, 2010, Oxygen and hydrogen diffusion in minerals: Reviews in Mineralogy and Geochemistry, v. **72**, n. 1, p. 447–507,doi:http://dx.doi.org/10.2138/rmg.2010.72.10
Farver J. R.,
Giletti B. J.
, 1989, Oxygen and strontium diffusion kinetics in apatite and potential applications to thermal history determinations: Geochimica et Cosmochimica Acta, v. **53**, n. 7, p. 1621–1631, doi:http://dx.doi.org/10.1016/0016-7037(89)90243-3
Ferry J. M.,
Passey B. H.,
Vasconcelos C.,
Eiler J. M.
, 2011, Formation of dolomite at 40–80° C in the Latemar carbonate buildup, Dolomites, Italy, from clumped isotope thermometry: Geology, v. **39**, n. 6, p. 571–574, doi:http://dx.doi.org/10.1130/G31845.1
Finnegan S.,
Bergmann K.,
Eiler J. M.,
Jones D. S.,
Fike D. A.,
Eisenman I.,
Hughes N. C.,
Tripati A. K.,
Fischer W. W.
, 2011, The magnitude and duration of Late Ordovician-Early Silurian glaciation: Science, v. **331**, n. 6019, p. 903–906,doi:http://dx.doi.org/10.1126/science.1200803
Ghosh P.,
Adkins J.,
Affek H.,
Balta B.,
Guo W.,
Schauble E. A.,
Schrag D.,
Eiler J. M.
, 2006, ^{13}C–^{18}O bonds in carbonate minerals: A new kind of paleothermometer: Geochimica et Cosmochimica Acta, v. **70**, n. 6, p. 1439–1456,doi:http://dx.doi.org/10.1016/j.gca.2005.11.014
Green P. F.,
Duddy I. R.,
Gleadow A. J. W.,
Tingate P. R.,
Laslett G. M.
, 1986,Thermal annealing of fission tracks in apatite: 1. A qualitative description: Chemical Geology: Isotope Geoscience section, v. **59**, p. 237–253,doi:http://dx.doi.org/10.1016/0168-9622(86)90074-6
Guo W.,
Mosenfelder J. L.,
Goddard W. A. III.,

Eiler J. M.
, 2009, Isotopic fractionations associated with phosphoric acid digestion of carbonate minerals: Insights from first-principles theoretical modeling and clumped isotope measurements:Geochimica et Cosmochimica Acta, v. **73**, n. 24, p. 7203–7225,doi:http://dx.doi.org/10.1016/j.gca.2009.05.071
Haynes E. A.,
Moecher D. P.,
Spicuzza M. J.
, 2002, Oxygen isotope composition of carbonates, silicates, and oxides in selected carbonatites: Constraints on crystallization temperatures of carbonatite magmas: Chemical Geology, v. **193**, n. 1–2, p. 43–57, doi:http://dx.doi.org/10.1016/S0009-2541(02)00244-9
Henkes G. A.,
Passey B. H.,
Grossman E. L.,
Shenton B. J.,
Pérez-Huerta A.,
Yancey T. E.
, 2014, Temperature limits for preservation of primary calcite clumped isotope paleotemperatures: Geochimica et Cosmochimica Acta, v. **139**, p. 362–382,doi:http://dx.doi.org/10.1016/j.gca.2014.04.040
Huntington K. W.,
Eiler J. M.,
Affek H. P.,
Guo W.,
Bonifacie M.,
Yeung L. Y.,
Thiagarajan N.,
Passey B.,
Tripati A.,
Daëron M.,
Came R.
, 2009, Methods and limitations of 'clumped' CO_2 isotope (Δ_{47}) analysis by gas-source isotope ratio mass spectrometry: Journal of Mass Spectrometry, v. **44**, n. 9, p. 1318–1329,doi:http://dx.doi.org/10.1002/jms.1614
Ihinger P. D.
, ms, 1991, *An experimental study of the interaction of water with granitic melt*: Pasadena, California, California Institute of Technology, Ph. D. thesis,190 p.
Jaffrés J. B. D.,
Shields G. A.,
Wallmann K.
, 2007, The oxygen isotope evolution of seawater: A critical review of a long-standing controversy and an improved geological water cycle model for the past 3.4 billion years: Earth-Science Reviews, v. **83**, n. 1–2, p. 83–122, doi:http://dx.doi.org/10.1016/j.earscirev.2007.04.002
Kapustin Y. L.
, 1986, The origin of early calcitic carbonatites: International Geology Review, v. **28**, n. 9, p. 1031–1044, doi:http://dx.doi.org/10.1080/00206818609466346
Kasting J. F.,
Howard M. T.,
Wallmann K.,
Veizer J.,
Shields G.,
Jaffrés J.
, 2006,Paleoclimates, ocean depth, and the oxygen isotopic composition of seawater: Earth and Planetary Science Letters, v. **252**, n. 1–2, p. 82–93,doi:http://dx.doi.org/10.1016/j.epsl.2006.09.029
Keating-Bitonti C. R.,
Ivany L. C.,
Affek H. P.,
Douglas P.,
Samson S. D.
, 2011,Warm, not super-hot, temperatures in the early Eocene subtropics: Geology, v. **39**, n.8, p. 771–774, doi:http://dx.doi.org/10.1130/G32054.1
Khan M. A.,
Raza H. A.
, 1986, The role of geothermal gradients in hydrocarbon exploration in Pakistan: Journal of Petroleum Geology, v. **9**, n. 3, p. 245–258,doi:http://dx.doi.org/10.1111/j.1747-5457.1986.tb00388.x
Koch P. L.,
Tuross N.,

Fogel M. L.
, 1997, The effects of sample treatment and diagenesis on the isotopic integrity of carbonate in biogenic hydroxylapatite: Journal of Archaeological Science, v. **24**, n. 5, p. 417–430,doi:http://dx.doi.org/10.1006/jasc.1996.0126
Kohn M. J.,
Cerling T. E.
, 2002, Stable isotope compositions of biological apatite, *in*Kohn M. J., Rakovan J. M., Huges J. M., editors, Phosphates—Geochemical, Geobiological, and Materials Importance: Reviews in Mineralogy and Geochemistry, v.**48**, n. 1, p. 455–488, doi:http://dx.doi.org/10.2138/rmg.2002.48.12
Kolodny Y.,
Kaplan I.
, 1970, Carbon and oxygen isotopes in apatite CO_2 and co-existing calcite from sedimentary phosphorite: Journal of Sedimentary Research, v.**40**, n. 30, p. 954–959.
Kronenberg A. K.,
Yund R. A.,
Giletti B. J.
, 1984, Carbon and oxygen diffusion in calcite: Effects of Mn content and P_{H2O}: Physics and Chemistry of Minerals, v. **11**, n.3, p. 101–112, doi:http://dx.doi.org/10.1007/BF00309248
Labotka T. C.,
Cole D. R.,
Riciputi L. R.
, 2000, Diffusion of C and O in calcite at 100 MPa: American Mineralogist, v. **85**, p. 488–494.
Labotka T. C.,
Cole D. R.,
Riciputi L. R.,
Fayek M.
, 2004, Diffusion of C and O in calcite from 0.1 to 200 MPa: American Mineralogist, v. **89**, p. 799–806.
Labotka T. C.,
Cole D. R.,
Fayek M. J.,
Chacko T.
, 2011, An experimental study of the diffusion of C and O in calcite in mixed CO_2-H_2O fluid: American Mineralogist, v.**96**, n. 8–9, p. 1262–1269, doi:http://dx.doi.org/10.2138/am.2011.3738
Lécuyer C.,
Allemand P.
, 1999, Modelling of the oxygen isotope evolution of seawater: Implications for the climate interpretation of the $\delta^{18}O$ of marine sediments:Geochimica et Cosmochimica Acta, v. **63**, n. 3–4, p. 351–361,doi:http://dx.doi.org/10.1016/S0016-7037(98)00277-4
Lloyd M.,
Eiler J.
, 2014, Laboratory and Natural Constraints on the Temperature Limit for Preservation of the Dolomite Clumped Isotope Thermometer: San Francisco,California American Geophysical Union Fall Meeting, p. 22
Longinelli A.,
Wierzbowski H.,
Di Matteo A.
, 2003, $\delta^{18}O(PO_4^{3-})$ and $\delta^{18}O(CO_3^{2-})$ from belemnite guards from Eastern Europe: Implications for palaeoceanographic reconstructions and for the preservation of pristine isotopic values: Earth and Planetary Science Letters, v. **209**, n. 3–4, p. 337–350,doi:http://dx.doi.org/10.1016/S0012-821X(03)00095-5
McClellan G. H.
, 1980, Mineralogy of carbonate fluorapatites: Journal of the Geological Society, v. **137**, n. 6, p. 675–681,doi:http://dx.doi.org/10.1144/gsjgs.137.6.0675
McCrea J. M.
, 1950, On the isotopic chemistry of carbonates and a paleotemperature scale: Journal of Chemical Physics, v. **18**, p. 849–857,doi:http://dx.doi.org/10.1063/1.1747785
Mitchell R. H.
, 2005, Carbonatites and carbonatites and carbonatites: The Canadian Mineralogist, v. **43**, n. 6, p. 2049–2068,doi:http://dx.doi.org/10.2113/gscanmin.43.6.2049
Muehlenbachs K.
, 1986, Alteration of the oceanic crust and the ^{18}O history of seawater: Reviews in Mineralogy and Geochemistry, v. **16**, p. 425–444.
Nadeau S. L.,
Epstein S.,
Stolper E.
, 1999, Hydrogen and carbon abundances and isotopic ratios in apatite from alkaline intrusive complexes, with a focus on carbonatites: Geochimica et Cosmochimica Acta, v. **63**, n. 11–12, p. 1837–1851,doi:http://dx.doi.org/10.1016/S0016-7037(99)00057-5

Passey B. H.,
Henkes G. A.
, 2012, Carbonate clumped isotope bond reordering and geospeedometry: Earth and Planetary Science Letters, v. **351–352**, p. 223–236,doi:http://dx.doi.org/10.1016/j.epsl.2012.07.021
Passey B. H.,
Levin N. E.,
Cerling T. E.,
Brown F. H.,
Eiler J. M.
, 2010, High-temperature environments of human evolution in East Africa based on bond ordering in paleosol carbonates: *Proceedings of the National Academy of Sciences of the United States of America*, v. **107**, n. 25, p. 11245,doi:http://dx.doi.org/10.1073/pnas.1001824107
Peters N. A.,
Huntington K. W.,
Hoke G. D.
, 2013, Hot or not? Impact of seasonally variable soil carbonate formation on paleotemperature and O-isotope records from clumped isotope thermometry: Earth and Planetary Science Letters, v. **361**, p. 208–218, doi:http://dx.doi.org/10.1016/j.epsl.2012.10.024
Price G. D.,
Passey B. H.
, 2013, Dynamic polar climates in a greenhouse world: Evidence from clumped isotope thermometry of Early Cretaceous belemnites:Geology, v. **41**, n. 8, p. 923–926, doi:http://dx.doi.org/10.1130/G34484.1
Quade J.,
Eiler J.,
Daeron M.,
Achyuthan H.
, 2013, The clumped isotope geothermometer in soil and paleosol carbonate: Geochimica et Cosmochimica Acta, v.**105**, p. 92–107, doi:http://dx.doi.org/10.1016/j.gca.2012.11.031

Schauble E. A.,
Ghosh P.,
Eiler J. M.
, 2006, Preferential formation of ^{13}C-^{18}O bonds in carbonate minerals, estimated using first-principles lattice dynamics:Geochimica et Cosmochimica Acta, v. **70**, n. 10, p. 2510–2529,doi:http://dx.doi.org/10.1016/j.gca.2006.02.011
Shemesh A.,
Kolodny Y.,
Luz B.
, 1983, Oxygen isotope variations in phosphate of biogenic apatites, II. Phosphorite rocks: Earth and Planetary Science Letters, v. **64**, n.3, p. 405–416, doi:http://dx.doi.org/10.1016/0012-821X(83)90101-2

Shemesh A.,
Kolodny Y.,
Luz B.
, 1988, Isotope geochemistry of oxygen and carbon in phosphate and carbonate of phosphorite francolite: Geochimica et Cosmochimica Acta, v. **52**, n. 11, p. 2565–2572, doi:http://dx.doi.org/10.1016/0016-7037(88)90027-0
Shuster D. L.,
Flowers R. M.,
Farley K. A.
, 2006, The influence of natural radiation damage on helium diffusion kinetics in apatite: Earth and Planetary Science Letters, v.**249**, n. 3–4, p. 148–161, doi:http://dx.doi.org/10.1016/j.epsl.2006.07.028
Silverman S. R.,
Fuyat R. K.,
Weiser J. D.
, 1952, Quantitative determination of calcite associated with carbonate-bearing Apatites: American Mineralogist, v. **37**, n. 3–4, p. 211–222.
Snell K. E.,
Thrasher B. L.,
Eiler J. M.,
Koch P. L.,
Sloan L. C.,
Tabor N. J.
, 2013,Hot summers in the Bighorn Basin during the early Paleogene: Geology, v. **41**, n. 1, p.55–58, doi:http://dx.doi.org/10.1130/G33567.1
Stolper D. A.,
Sessions A. L.,

Ferreira A. A.,
Santos Neto E. V.,
Schimmelmann A.,
Shusta S. S.,
Valentine D. L.,
Eiler J. M.
, 2014, Combined ^{13}C-D and D-D clumping in methane: Methods and preliminary results: Geochimica et Cosmochimica Acta, v. **126**, p. 169–191, doi:http://dx.doi.org/10.1016/j.gca.2013.10.045
Swart P. K.,
Burns S. J.,
Leder J. J.
, 1991, Fractionation of the stable isotopes of oxygen and carbon in carbon dioxide during the reaction of calcite with phosphoric acid as a function of temperature and technique: Chemical Geology: Isotope Geoscience section, v. **86**, n. 2, p. 89–96, doi:http://dx.doi.org/10.1016/0168-9622(91)90055-2

Taylor H. P. Jr..,
Frechen J.,
Degens E. T.
, 1967, Oxygen and carbon isotope studies of carbonatites from the Laacher See district, West Germany and the Alnö district, Sweden: Geochimica et Cosmochimica Acta, v. **31**, n. 3, p. 407–430,doi:http://dx.doi.org/10.1016/0016-7037(67)90051-8

M.,
Grosche G.,
Götze J.,
Belyatsky B. V.,
Savva E. V.,
Keller J.,
Todt W.
, 2006, The mineral isotope composition of two Precambrian carbonatite complexes from the Kola Alkaline Province — Alteration versus primary magmatic signatures: Lithos, v. **91**, n. 1–4, p. 229–249,doi:http://dx.doi.org/10.1016/j.lithos.2006.03.019
Urey H. C.
, 1947, The thermodynamic properties of isotopic substances: Journal of the Chemical Society, p. 562–581, doi:http://dx.doi.org/10.1039/jr9470000562
Veizer J.,
Ala D.,
Azmy K.,
Bruckschen P.,
Buhl D.,
Bruhn F.,
Carden G. A. F.,
Diener A.,
Ebneth S.,
Godderis Y.,
Jasper T.,
Korte C.,
Pawellek F.,
Podlaha O. G.,
Strauss H.
, 1999, ^{87}Sr/^{86}Sr, δ^{13}C and δ^{18}O evolution of Phanerozoic seawater:Chemical Geology, v. **161**, n. 1–3, p. 59–88, doi:http://dx.doi.org/10.1016/S0009-2541(99)00081-9
Wang Z.,
Schauble E. A.,
Eiler J. M.
, 2004, Equilibrium thermodynamics of multiply substituted isotopologues of molecular gases: Geochimica et Cosmochimica Acta, v.**68**, n. 23, p. 4779–4797, doi:http://dx.doi.org/10.1016/j.gca.2004.05.039
Wyllie P. J.,
Tuttle O. F.
, 1960, The system CaO-CO_2-H_2O and the origin of carbonatites: Journal of Petrology, v. **1**, n. 1, p. 1–46,doi:http://dx.doi.org/10.1093/petrology/1.1.1
Yeung L. Y.,
Young E. D.,
Schauble E. A.

, 2012, Measurements of $^{18}O^{18}O$ and $^{17}O^{18}O$ in the atmosphere and the role of isotope-exchange reactions: Journal of Geophysical Research-Atmospheres, v. **117**, n. D18,doi:http://dx.doi.org/10.1029/2012JD017992
Zaarur S.,
Affek H. P.,
Brandon M. T.
, 2013, A revised calibration of the clumped isotope thermometer: Earth and Planetary Science Letters, v. **382**, p. 47–57,doi:http://dx.doi.org/10.1016/j.epsl.2013.07.026
Zhabin A. G.
, 1971, Primary textural-structural features of carbonatites and their metamorphic evolution: International Geology Review, v. **13**, n. 7, p. 1087–1096,doi:http://dx.doi.org/10.1080/00206817109475540
Zhang Y.
, 1994, Reaction kinetics, geospeedometry, and relaxation theory: Earth and Planetary Science Letters, v. **122**, n. 3–4, p. 373–391,doi:http://dx.doi.org/10.1016/0012-821X(94)90009-4
Zhang Y.
, 2008, *Geochemical Kinetics*: Princeton, New Jersey, Princeton University Press, 644 p.
Zhang Y.,
Stolper E. M.,
Ihinger P. D.
, 1995, Kinetics of the reaction $H_20+ 0= 20H$ in rhyolitic and albitic glasses: Preliminary results: American Mineralogist, v. **80**, n. 5–6, p. 593–612.